Submitted to Nucl. Phys.

LNF-91/058 (P)
2 Settembre 1991

A.S. Iljinov, M.V. Mebel and N. Bianchi, E. De Sanctis, C. Guaraldo, V. Lucherini, V. Muccifora, E. Polli, A.R. Reolon, P. Rossi:

PHENOMENOLOGICAL STATISTICAL ANALYSIS OF LEVEL DENSITIES, DECAY WIDTHS AND TIME LIVES OF EXCITED NUCLEI

INFN - Laboratori Nazionali di Frascati
Servizio Documentazione

LNF-91/058 (P)
2 Settembre 1991

PHENOMENOLOGICAL STATISTICAL ANALYSIS OF LEVEL DENSITIES, DECAY WIDTHS AND TIME LIVES OF EXCITED NUCLEI

A.S. Iljinov and M.V. Mebel
Institute for Nuclear Research of the Academy of Sciences of the USSR, Moscow 117312, USSR

N. Bianchi, E. De Sanctis, C. Guaraldo, V. Lucherini, V. Muccifora, E. Polli, A.R. Reolon, and P. Rossi(*) .
INFN – Laboratori Nazionali di Frascati, I – 00044 Frascati, Italy

ABSTRACT: All existing data on the level densities, decay widths and time lives of excited nuclei have been analyzed in the framework of the statistical model in order to better determine the parameters of the phenomenological systematics of the nuclear level density. Data on level densities of several hundred nuclides obtained in the excitation energy range from 2 MeV up to 20 MeV were used. The level densities of nuclei with large deformation (at the saddle point) have been studied by analyzing the data on the neutron emission and fission partial width ratio Γ_n/Γ_f, and the values of the fission barrier heights B_f, the level density parameters ratio a_f/a_n and the saddle point shell corrections δW_{sp} have been extracted. The influence of shell and collective effects on the level density and the decay widths of nuclei which have different excitation energies and deformations has been studied.

PACS No 21.10.Ma; 23.20.Ck

1. INTRODUCTION

Residual nuclei with excitation energy U up to 100 MeV and higher can be produced in deep inelastic interactions of intermediate energy particles with nuclei.[1] To describe the deexcitation of these highly excited nuclei, a statistical approach is usually applied. In this approach the more important quantity of the model is the nuclear level density.[2-4] In fact, nuclear reactions initiated by intermediate energy particles have a specific feature, in that residual nuclei have a wide distribution over the excitation energy (U) and over the neutron (N) and proton (Z) numbers. In addition, the

(*) Permanent address: INFN- Sezione Sanitá, Viale Regina Elena 299, 00100 Roma

emission of particles from the residual nucleus, during the steps of the evaporation chain, involves the production of intermediate nuclei, which have excitation energies varying from $U<B_n$ (B_n being the neutron binding energy) up to the initial value. These nuclei decay to the ground state through emission of particles and photons. Moreover, at each step of the evaporation cascade they can undergo fission. The characteristics of various decay modes are determined by the competition between emission particles and fission, and thus by the values of the partial widths of corresponding channels. So one needs a sufficiently accurate description of the nuclear level density over a wide interval of the excitation energies and nuclear composition, of the fission barrier heights, of the level density parameters and of the shell corrections of the nuclei at the saddle point.

A lot of experimental information on the properties and decay of compound nuclei with excitation energies in the interval from several MeV up to ~10^2 MeV produced in low energy nuclear reactions has been accumulated in literature. These data constitute a good basis for updating the statistical evaporation model,[3,4] by taking into account more accurately both the influence of shell effects on different characteristics of the evaporation process and the thermal damping of the shell effects in nuclei.

In this paper we analyze the total bulk of data on level density, decay widths and time-lives of excited compound nuclei in the framework of the statistical approach. The aim of this work was to reduce the uncertainties of the parameters of the evaporation model by analyzing this large set of experimental data now available on the level densities, decay widths and time lives of excited nuclei produced in low energy nuclear reactions. The more accurate determination of these parameters will allow to use this model as a part of the combined cascade-evaportion approach to describe more correctly the yields of the low energy secondaries and isotopes, and the fission cross-sections in intermediate energy nuclear reactions and to obtain more reliable information about the mechanism of formation of hot nuclei in the deep inelastic interaction of intermediate energy particles with nuclei.

This paper is divided into two parts relevant, respectively, to nuclear level density, decay widths, and time-lives of excited nuclei. Specifically, in Section 2 we provide a brief overview of the formulae used to describe the nuclear level density, we discuss the procedure used to determine the phenomenological systematics from data and the influence of shell and collective effects on the evaporation process and we compare our systematics results with data. In Section 3 we give a brief overview of formulae relevant to decay widths, describe experimental data on neutron resonance radiative widths, fissilities and time lives of excited nuclei with the aid of the phenomenological systematics.

2. NUCLEAR LEVEL DENSITY

2.1 The main expressions for the nuclear level density

In the adiabatic approximation for the selection between rotational and vibrational modes, the nuclear level density $\rho(U)$ is generally described by the following expression:[4, 15]

$$\rho(U) = K_{rot}K_{vib}\rho_{int}(U), \quad (1)$$

where K_{rot} and K_{vib} are the coefficients for rotational and vibrational enhancement of the non-collective internal nuclear excitations $\rho_{int}(U)$. To describe this quantity, one often uses the Fermi-gas expression:[2-4]

$$\rho_{int}(U) = \frac{\sqrt{\pi}}{12} a^{-1/4} (U-\Delta)^{-5/4} exp\left(2\sqrt{a(U-\Delta)}\right), \quad (2)$$

where a is the level density parameter, and

$$\Delta = \chi \frac{12}{\sqrt{A}} \text{ [in MeV]}, \quad (3)$$

is the pairing energy (χ=0,1, or 2, respectively for odd-odd, odd-even, or even-even nuclei). The experimental data extracted from the neutron resonances show that this parameter at the excitation energy $U \approx B_n$ is strongly influenced by the shell effects.[3,4] In fact, it was straightforward to connect the observed anomalies in the A-dependence of the level density parameter with the value of the shell correction in the nuclear mass formula $\delta W_g(Z,N)$[5] or with the filling of nucleon shells with increasing A.[6] On the contrary, in the Fermi-gas model this parameter depends only on the mass number: $a=\alpha A$, with α=const.[2-4] Therefore, the empirical approximations[5,6] based on these assumptions are able to describe the experiment in the narrow energy interval $U \approx B_n$, but do not allow to extrapolate the value of the level density up to the high energy region. This means that shell effects are assumed to manifest themselves in the level density at high energies in the same manner as at low energies.

Another empirical approximation, the back–shifted Fermi-gas model,[7,8] also uses the same assumption.

The development of numerical methods[9,10] to calculate the nuclear level density using single particle level scheme of the shell model allowed to understand how these effects manifest themselves at different values of nuclear excitation. In particular, it was shown that shell effects are strongest at low excitation energies, and disappear at U>50 MeV.[3,4] However, it is difficult to calculate correctly the absolute values of the level densities of highly excited nuclei due to uncertainties on the nuclear potential, and on the understanding of the formation of the nuclear states from the single particle states. Moreover, microscopic calculations are rather complicated to include them into the evaporation calculations.

Afterwards, a phenomenological method was developed[11] to calculate correctly the absolute values of the nuclear level density. In this method the function which describes the thermal damping of shell effects (i.e. the energy dependence of the parameter a) was taken from the microscopic shell model calculations, and the parameters were adjusted to reproduce correctly the data on the absolute values of the nuclear level density. This method unifies the advantages of the previous methods of

calculations of the nuclear level density, namely: the simplicity of the Fermi-gas expression (2), the high accuracy of the absolute values of the level density, the consideration of the damping of shell effects with increasing the excitation energy, and the possibility of performing a reliable extrapolation to high excitation region. Therefore, in our work we selected this method which is suitable for using in the evaporation calculations.

The semiempirical approach of ref. [11] is based on the following relation which describes the dependence of the level density parameter on the shell correction in the nuclear mass formula and on the excitation energy:

$$a(U, Z, N) = \tilde{a}\ (A)\left\{ 1+ \delta W_g(Z, N)\frac{f(U - \Delta)}{U-\Delta}\right\}, \qquad (4)$$

where:

$$\tilde{a}\ (A) = \alpha\, A + \beta\, A^{2/3}\, b_s, \qquad (5)$$

is the asymptotic Fermi-gas value of the level density parameter at high excitation energy. (The term proportional to the nuclear surface is due to the existence of gradients of the nucleon density distribution in the nucleus; β is a constant, and the factor b_s is the surface area of the nucleus in units of the surface for the sphere of equal volume. For the ground state of nucleus $b_s \approx 1$). The shape of the function f(U), which defines the energy dependence of the level density parameter, was found by approximation of the numerical microscopical calculations based on the shell model:

$$f\ (U) = 1 - exp\ (-\gamma U). \qquad (6)$$

This energy dependence was assumed[11] to be a universal one for all nuclei, moreover with the γ parameter constant. On the contrary, other authors[12] assumed this parameter to be A-dependent, since it is connected with the asymptotic level density parameter by the relation:

$$\gamma = \frac{\tilde{a}}{\varepsilon\ A^{4/3}}. \qquad (7)$$

(being ε is a phenomenological parameter). Moreover the microscopic shell model calculations[13] showed that the shape of the function f(U) may be influenced by the individual peculiarities of the single particle level scheme of the given nucleus.

As said at the beginning, the level density is strongly influenced by the collective effects. The collective enhancement of the level density is especially large in the case of deformed nuclei. The coefficient of rotational increase of the level density is defined by expression:[4,15]

$$K_{rot} = \begin{cases} 1 & \text{for spherical nuclei} \\ \theta_{\perp} \cdot T & \text{for deformed nuclei} \end{cases}, \qquad (8)$$

where $T=\sqrt{(U-\Delta)/a}$ is the nuclear temperature, $\theta_{\perp} = \theta_{r.b.} f(\beta_2,\beta_4)$ is the perpendicular moment of inertia, $\theta_{r.b.}=0.4MR^2$ is the rigid body moment of inertia, M and R are the mass and the radius of the nucleus, $f(\beta_2,\beta_4)= [(1+\sqrt{\frac{5}{16\pi}}\,\beta_2 + \frac{45}{28\pi}\beta_2^2 + \frac{15}{7\pi\sqrt{5}}\beta_2\beta_4)]$, β_2 and β_4 are the parameters of quadrupole and octupole deformations of the nucleus.[16] The liquid drop model estimation for the vibrational coefficient is:[4]

$$K_{vib} \approx exp\ (0.0555\ A^{2/3}\ T^{4/3})\ . \qquad (9)$$

The rotational enhancement of the level density of deformed nuclei $K_{rot}\approx(10\div10^2)$ is considerably larger than the vibrational enhancement $K_{vib}\approx3$ at energy $U\approx B_n$.

2.2 Experimental data on the nuclear level density and extraction of parameters of the systematics $\rho(U)$

We determined the values of the parameters α, β, and γ (or ε) of the phenomenological systematic $\rho(U)$ from a least squares fit to experimental data on the nuclear level density on the basis of equations (1)–(7). As usual, the experimental data on the nuclear level density, $\rho_{exp}(U)$, were derived from the observed level spacing resonance spacing D_{obs} by the relation:[3]

$$\frac{1}{\rho_{exp}(U)} = \frac{D_{obs}}{4\sigma^2} \sum_{(I^{\pi})_{obs}} (2I^{\pi}+1)\ exp\left[-\frac{(I^{\pi}+\frac{1}{2})^2}{2\sigma^2}\right]. \qquad (10)$$

Here the symbol $(I^{\pi})_{obs}$ denotes that the sum extends over all possible combinations of spin and parity (I and π) of nuclear levels. The spin-cutoff parameter is usually calculated by the formula $\sigma^2=T\cdot\theta_{r.b.}/\hbar^2$, using the value $R=r_0\cdot A^{1/3}$ for the nuclear radius (being $r_0=1.2$ fm) .

The expression (10) is a consequence of the relation existing between the level density $\rho(U,I)$ of nucleus having angular momentum I and excitation energy U, and the total level density $\rho(U)$:[2,3]

$$\rho\ (U,I) = \frac{2I+1}{2\sqrt{2\pi}\ \sigma^3} exp\ [-\frac{(I+\frac{1}{2})^2}{2\sigma^2}]\ \rho(U)\ . \qquad (11)$$

The most large and reliable information on the level density has been accumulated from measurements of neutron resonances. For s-resonances (neutron angular momentum equal to 0) we obtained, from the equation (10) and (11), the equations:

$$\begin{cases} \rho_{exp}(U, I=1/2) = 2/D_{obs} & \text{for } s = 0 \\ \rho_{exp}(U,s+1/2) + \rho_{exp}(U,s-1/2) = 2/D_{obs} & \text{for } s \neq 0 \end{cases}, \qquad (12)$$

which we used to extract the experimental values of the level density parameter a_{exp} from the neutron resonance spacings D_{obs}. Here, I is the total angular momentum of the compound nucleus, and s is the spin of the target nucleus. The excitation energy of the compound nucleus formed after thermal neutron capture is $U \approx B_n$. Values of the neutron binding energy B_n were taken from the mass Tables[17].

Table I contains the initial data[5,7,8,18 -25] on neutron resonance spacing and the results of the analysis we performed by using the relationship (12). Table I includes those data for 284 nuclides which satisfy the following criteria: *(i)* s-wave neutron resonace spacing available; *(ii)* sufficiently large number ($\geq 5 \div 10$) of observed resonances for a given nuclide; and *(iii)* measurements for a given nuclide performed at least by two different experimental groups.

Unlike the refs. [4,11], where the neutron resonance data were used to determine the parameters of the semiempirical systematics for the level density, the present paper involves also the data obtained both at high and low excitation energies U. This enlargement of the energy interval allowed us to extract more reliable information about the function (6) which describes the thermal damping of shell effects. We obtained level densities at the lowest energies from data counting low-lying bound levels, and, at higher energies, from level spacing data from several reactions [(γ,n), (p,γ), (p,p'), (p,α), (α,γ), (α,n), (d,p), (^{3}He, d), (^{3}He, α)]. As different angular momenta l = 0,1,2.... are involved in these reactions, we performed the summation in (11) over all angular momentum values I of populated levels when we analyzed these data. In this case, as it is follows from expression (11), the observed level density $\rho_{exp}(U)$ is connected with the total level density (state density) by the relation:

$$\rho_{exp}(U) = \sum_I \rho(U,I) \approx \frac{\rho(U)}{\sqrt{2\pi}\,\sigma}. \qquad (13)$$

Table II contains the 228 experimental values of the level density we used.[7,26-33] These data satisfy the following criteria: *(i)* nuclear excitation energy $(U-\Delta) \geq 2$ MeV, and *(ii)* absolute values $\rho(U \approx B_n)$ consistent with neutron resonance data. Moreover, Table II includes results of the Ericson fluctuation measurements.

2.3 Shell effects in nuclear level density

In Fig. 1 are shown the experimental values of the level density parameter a_{exp} we derived for different nuclides. As it is seen, clear structures are evident: these structures correlate unambiguously with similar structures in the A-dependence of the shell correction in the nuclear mass $\delta W_g(Z,N)$. So

the level density parameter are strongly influenced by shell effects at $U \approx B_n$. As a consequence, the parameters of the semiempirical systematics of nuclear level density depend on the "empirical" shell correction used in the fitting procedure of the data. The "empirical" shell correction was determined by the relationship:

$$\delta W_g(A,Z,\beta) = M_{exp}(A,Z) - M_{LD}(A,Z,\beta_0), \tag{14}$$

where $M_{LD}(A,Z,\beta_0)$ is the liquid drop part in the mass formula for the nuclear equilibrium deformation β_0.

In this paper we used two sets of empirical shell corrections in the nuclear mass formulae. The first, by Myers and Swiatecki[34] (M-S), corresponds to generally accepted definition of liquid drop model parameters which is wide-spread used in the description of nuclear fission. The second, by Cameron[35] (C), presents the shell correction in the form of a table $\delta W_g(A,Z) = [\delta W_g(N) + \delta W_g(Z)]$, which is convenient for numerical calculation of evaporation cascade. As shown in Fig. 1 the discrepancy in absolute values of shell corrections for these two sets may amount up to 2 MeV.

The parameters we obtained for different variants of the phenomenological systematics, which corresponds to different ways of taking into account shell and collective effects, different A–dependences of the level density parameter *a*, etc., are presented in Table III. To give a quantitative overall estimation of the agreement between calculation and experimental data on the level density, the averaged ratio (*f*-factor in the following):

$$f \equiv \left\langle \frac{\rho_{calc}}{\rho_{exp}} \right\rangle = exp\left[\frac{1}{n} \sum_{i=1}^{n} \left(ln \frac{\rho^i_{calc}}{\rho^i_{exp}} \right)^2 \right]^{1/2} \tag{15}$$

is usually used,[5,23] where n is the number of experimental points. Values of the factor f are also given in Table III.

From Table III (case without collective effects) one sees that: *(i)* the systematics based on M-S shell corrections[34] describes experiments better than systematics based on C shell corrections[35] (they have lower f values); *(ii)* there is a deviation from the linear dependence of the Fermi-gas level density parameter $\tilde{a}$ on the mass number A; *(iii)* the description of data is not improved if the A-dependence (7) of parameter γ is taken into account (one has f=1.71 instead of 1.68). Moreover, one should notice that the value of the parameter $\gamma = (0.05 \div 0.06)$ MeV^{-1}, which defines the rate of damping of shell effects, agrees well with the value $\gamma = 0.05$ MeV^{-1} obtained by the microscopic shell model calculations;[4,11] *(iv)* the empirical value the parameter ε=0.46, for the variant which takes into account the A-dependence (7) of the parameter γ, is close to the theoretical estimation, ε=0.4.[12]

From what said above, we will use the parameters of the systematics with M-S shell corrections and with parameter γ independent of the mass number A.

2.4 Collective effects in nuclear level density

In order to take into account the collective enhancement of the nuclear level density in the phenomenological systematics, it is important to know whether a given nucleus is spherical or deformed. In fact, a strong rotational enhancement of the level density starts its influence at the same time as a nuclear deformation appears (see condition (8)).

In Fig. 2 (a) we give the asymptotic value of the level density parameter $\tilde{a}$ as a function of A obtained without taking into account rotational and vibrational enhancements (K_{rot}=1, and K_{vib}=1). As it is shown the A-dependence is correct but the $\tilde{a}$ values are considerably larger than experimental and theoretical results,[4,36,37] [that is about (A/7÷A/8) instead of about (A/10÷A/15)].

Assuming, as usual,[4] that all nuclides are spherical apart those lying in the regions 150<A<204, and A > 230, we obtained the results shown in Fig. 2 (b): that is, the A-dependence of the Fermi-gas parameter $\tilde{a}$ becomes to be unsmooth, and contradictory to the physical meaning of this parameter, and the agreement between calculations and data is bad (see Table III, case with collective effects).

Recent theoretical calculations[38] showed that practically all nuclides have non-zero equilibrium deformation at the ground state. Moreover, spherical nuclides in excited states may have properties of deformed nuclei due to the existence of dynamical deformation. Then, we assumed that all nuclides, for which experimental data are available, have collective enhancement on the level density, and we obtained the results shown in Fig. 2 (c). That is, our phenomenological approximation gives the required smooth dependence of $\tilde{a}$(A), and describes experiment rather well (see Table III). Moreover, the asymptotical values of the level density parameter $\tilde{a} \approx$ (A/10÷A/15) are reasonable from the physical point of view. It should be noted that, also in this case, the variant of systematics based on M-S shell corrections[34] describes experiments better than systematics based on C shell corrections[35] which corresponds to more fast thermal damping of shell effects.

2.5 Comparison of phenomenological systematics with data on level density

Here, we compare in more details the phenomenological systematics with experimental results. At first, we consider neutron resonance data. As it is seen from Figs. 3 and 4, our systematics reproduces correctly the details of the structure in the A-dependence as caused by shell effects and provides also an accurate calculation (within a factor 2) of the absolute values of the level density. Both variants of the systematics, with and without collective effects, are able to describe neutron resonance data measured at an excitation energy U≈B_n, because in this case we simply redetermine absolute values of level densities with help of expression (1).

Differences between the two variants of the systematics which have different asymptotic value of the parameter $\tilde{a}$ are shown in Figs. 5 and 6, where the energy dependences ρ(U) are displayed for the given nuclei, together with experimental data. In the case of light nuclei the variant of the systematics with the M-S shell corrections[34] describes data better than the variant with the C shell corrections.[35] Variant of the systematics with collective effects gives a weaker energy dependence

and describes the experiments better at higher excitations, U≈(20÷30) MeV. However, it is desirable to analyze other characteristics of decay of excited nuclei, in particular the decay widths, before drawing more definite conclusions about the phenomenological systematics of nuclear level density and developing a more correct evaporation model.

3. PARTIAL DECAY WIDTHS AND TIME LIVES OF EXCITED NUCLEI

3.1 The main relationships for particle decay widths of excited nuclei

For studying the level densities of nuclei with large deformation (at the saddle point) we analyzed the data on the neutron emission and fission partial width ratio Γ_n/Γ_f, and extracted the values of the fission barrier heights B_f, the level density parameters ratio a_f/a_n and the saddle point shell corrections δW_{sp}. In this case one has not access to the level density itself, but one is dealing with ratios of partial decay widths, which depend on the level density of compound and residual nuclei. This makes difficult the analysis and, in principle, decreases the sensitivity of data to the level densities studied. Nevertheless, data on decay widths allow to test the nuclear level density systematics on a wider energy interval, and, in some particular cases (for example, nuclear fissilities), to evidence more reliably the influence on the nuclear level density of shell and collective effects.

In the statistical model the following expressions[39,40] are generally used to calculate the partial widths Γ_j, Γ_γ, and Γ_f, respectively for the emission of a particle j (j ≡ n, p, d, t, ^{3}He, α), photon and fission:

$$\Gamma_j = \frac{g_j m_j}{(\pi\hbar)^2} \frac{1}{\rho_0(U_0)} \int_{V_j}^{U_j - B_j} \sigma_{inv}(E)\, \rho_j(U_j - B_j - E)\, E dE, \qquad (16)$$

$$\Gamma_f = \frac{1}{2\pi} \frac{1}{\rho_0(U_0)} \int_0^{U_f - B_f} \rho_f(U_f - B_f - E)\, dE\,. \qquad (17)$$

$$\Gamma_\gamma = \frac{1}{(\pi\hbar c)^2} \frac{1}{\rho_0\,(U_0)} \int_0^{U_0} \sigma_\gamma(E)\, \rho_\gamma(U_0 - E)\, E^2\, dE, \qquad (18)$$

Here, ρ_0, ρ_j, ρ_γ, and ρ_f are the level densities of compound nucleus and residual nuclei produced after the emission of the j–th particle, γ–quantum and at the fission saddle point, respectively; g_j, m_j, V_j, and B_j are the spin factor, the mass, the Coulomb barrier, and the binding energy of the j–th particle, respectively; B_f is the fission barrier height; $\sigma_{inv}(E)$ is the inverse cross-section for absorption of j–th particle or γ–quantum with kinetic energy E by the residual nucleus; $U_j=(U_{cn}-\Delta_j)$; $U_0=(U_{cn}-\Delta_0)$; $U_f=(U_{cn}-\Delta_f)$; U_{cn} is the excitation energy of the compound nucleus, Δ_0, Δ_j, and

$\Delta_f=14\chi/\sqrt{A}$ [in MeV] are the pairing energy for compound and residual nuclei, and also for fission saddle point(*).

Writing the series expansion for the integrand (16) near the upper limit and then performing integration with the energy dependence $\sigma_{inv}(E)=\sigma_{geom}c(1+d/E)$, (being c and d constants) one obtains[41] for the neutron emission width:

$$\Gamma_n \approx \frac{g_n\, m_n}{(\pi\hbar)^2}\sigma^n_{geom}\, c_n\, T_n\, \frac{\rho_n(U-B_n)}{\rho_0(U_0)}\left[T_n + d_n - (U-B_n+T_n+d_n)\, exp\,(-\frac{U-B_n}{T_n})\right], \qquad (19)$$

and for the charge particle emission width:

$$\Gamma_j \approx \frac{g_j\, m_j}{(\pi\hbar)^2}\,\sigma^j_{geom}\, c_j\, T_j\, \frac{\rho_j(U-B_j-V_j)}{\rho_0(U_0)}\,\left[T_j - (U-B_j-V_j+T_j)\, exp(-\frac{U-B_j-V_j}{T_j})\right]. \qquad (20)$$

The constants c_j and d_j in the inverse cross–section expression are taken from ref.[42] (remember that $\sigma^j_{geom}=\pi r_o^{\,2}\,(A-A_j)^{2/3}$). In a similar way one obtains for the fission width:

$$\Gamma_f \approx \frac{1}{2\pi}T_f\frac{\rho_f(U-B_f)}{\rho_0(U_0)}\left[1 - exp\left(-\frac{U-B_f}{T_f}\right)\right]. \qquad (21)$$

From the definition of temperature as: $T=\left(\frac{d\ ln\ \rho(U)}{dU}\right)^{-1}$, taking for $\rho(U)$ the forms (2), and (4), we obtained the expression for temperature in the j–th decay channel (j=n, p, d, t, ^{3}He, α, f):

$$T_j = (S_j - F_j)^{-1}, \qquad (22)$$

where: $S_j=\frac{\tilde{a}_j\, q_j}{a_j(U_j')\cdot U_j'}$; $F_j=\frac{1}{U_j'}(1+\frac{\tilde{a}_j\, q_j}{4\, a_j(U_j')})$; $q_j=(1+\frac{\gamma\,\delta W_j}{exp\,(\gamma U_j')})$; $U_j'=(U-B_j-V_j)$ for particle emission, and $U_f'=(U-B_f)$ for fission. We derived Γ_γ by numerical integration of expression (18). In this case, to describe the dipole photoabsorption cross-section we used the dependence:

$$\sigma_\gamma(E_\gamma) = \frac{\sigma_0 E_\gamma^2 \Gamma_R^2}{(E_\gamma^2-E_R^2)^2+\Gamma_R^2 E_\gamma^2}, \qquad (23)$$

here the empirical parameters of the giant dipole resonance have the values[43] $\sigma_0=2.5\cdot A$ [in mb], $\Gamma_R=0.3\cdot E_R$, and $E_R=40.3/A^{0.2}$ [in MeV].

(*) In the following we will use the notation U instead U–Δ not to overload formulae.

In the next paragraphs we analyze the experimental data on the basis of the relationships for Γ_j, Γ_γ, and Γ_f described above and the phenomenological systematics for nuclear level density.

3.2 Neutron resonance radiative width

Low energy neutron experiments allow to obtain a large information on the averaged resonance spacing and on the total averaged radiative width Γ_γ of neutron resonances. Fig. 7 shows experimental values of Γ_γ for 132 nuclides[44] together with the calculated ones. Both experimental and calculated A–dependences manifest a shell structure which is more evident nearby the closed shell N=126. The peak around A≈60 observed in the experimental data is absent in the calculated one. To this respect it should be noted that experimental errors at this region are very large.[44] It is noteworthy that spread of Γ_γ values for neighbouring nuclei lying between closed shells is larger in the calculation than in the experiment. The reason is that the phenomenological systematics takes into account the pairing effects via expressions (2) and (3) which give significant error at the level density calculation when $U<B_n$. To modify the phenomenological systematics in the region of low excitations, one generally uses relationships of the generalized superfluid model of the nucleus.[45]

Let us notice that the variant of systematics of the nuclear level density with M-S shell corrections, the surface term in the asymptotic parameter $\tilde{a}$, and the collective effects describes data on the total averaged radiative widths of neutron resonances better than other variants.

Moreover, Fig. 8 shows that this variant describes data on Γ_γ with sufficient accuracy (the average value of the factor $\lambda \equiv <\Gamma_\gamma^{exp}/\Gamma_\gamma^{calc}>$ is 1.78). The similar calculation with C shell correction has practically the same accuracy (λ=1.81); while calculation without collective effects gives Γ_γ values which are twice lower (λ=2.67). This is an additional proof in favour of the systematics which takes into account collective effects.

3.3 Nuclear fissility

A lot of experimental data are available on cross-section of fission of heavy nuclei (A≥ 170) induced by low energy particles.[45] As the main decay channels of excited heavy nuclei are neutron emission and fission, from these data one extracts the energy dependence of the ratio of the partial widths Γ_f/Γ_n and, using expressions (16-21), it is possible to study the nuclear level density at the fission saddle point.

In this case the nucleus has the maximum possible deformation and collective effects influence the nuclear level density strongly. Moreover, the analysis of the energy dependence of the ratio Γ_f/Γ_n allows to investigate the influence of the shell effects on the nuclear level density in a relatively large region of excitation energies and deformations of the nucleus.

From this point of view it is interesting to study the fissility of nuclei in two regions of the nuclide chart, specifically those of preactinide and transuranium nuclei. In fact, nuclei nearby lead have a maximum deformation (dumb-bells shape) at the saddle point. A large shell correction in the

ground state influences strongly the level density in the neutron channel and leads to a high fission barrier height B_f. As a result, fissility of preactinides is sensitive to both collective and shell effects in nuclei which have an equilibrium deformation. Actinides have a double-humped structure of fission barrier due to strong oscillation of shell correction with deformation. The fission barrier height B_f of the heaviest transuranium nuclei is exhausted by the shell component. So fissility of actinides is sensitive to shell effects at the fission barrier, and energy dependence of fissility is sensitive to velocity of damping of shell effects with excitation energy.

3.3.1 Fissility of preactinide nuclei

Once the level density parameters of a nucleus in the neutron channel are obtained from data on ρ, then the Γ_f/Γ_n ratio depends mainly on two parameters, specifically on the fission barrier height B_f and the level density parameter ratio of the nucleus at the saddle point a_f/a_n.

The fission barrier height B_f is connected with its liquid-drop component B_f^{LD}, and with the shell corrections of the nucleus at the ground state δW_g and at the saddle point δW_{sp} through the expression:

$$B_f = B_f^{LD} - \delta W_g + \delta W_{sp}. \qquad (24)$$

Usually, one neglects the shell correction at the saddle point of preactinides ($\delta W_{sp} \approx 0$).[45] In fact, the shell component in the nuclear potential energy is assumed to be small ($\delta W_{sp} \leq 1$ MeV) because the nucleus has a maximum possible deformation at the saddle point, and this configuration is close to the scission configuration in the case of preactinides. Due to the manifestation of the shell structure in the nuclear ground state (nuclides near lead have shell correction $\delta W_g \approx -10$ MeV), the fission barrier heights of preactinides are increasing and amount to a value $B_f \approx 20$ MeV when we approach to the closed shell N = 126.

Considerable difference in the deformations of a nucleus at equilibrium and transitional states must lead to higher value of the asymptotical level density parameter ratio of the nucleus at the saddle point than at the ground state: $\tilde{a}_f/\tilde{a}_n > 1$ (see expression (5) and remember that $b_s \approx 2^{1/3}$ for saddle point of preactinides[45]).

We analyzed Γ_f/Γ_n data given in ref. [45] on the basis of expressions (16-21) and we adjusted the parameters B_f, $\tilde{a}_f/\tilde{a}_n$, and δW_{sp} to achieve the best agreement between calculation and experiment.(*) The procedure of adjusting the parameters was formulated taking into account the peculiarity of preactinide fission, namely strong dependence of fission probability on excitation energy. Due to this fact, the position of the fission threshold B_f is defined by the position of the sharp drop of Γ_f/Γ_n caused by the decreasing of the transmission through the fission barrier at energies near B_f. Therefore, the determination of the B_f value does not strongly depend on the model description of the level density in the neutron and fission channels. So at first we derived the fission barrier height

(*) More strictly, from experimental data one extracts Γ_f/Γ_{tot} instead of Γ_f/Γ_n.

B_f from the description of experimental ratios Γ_f/Γ_n in the region of the lowest energies U, then, to describe experimental points at higher energies, we adjusted the other important parameter $\tilde{a}_f/\tilde{a}_n$. Finally, if it was impossible to achieve a good description of experiment, we adjusted the parameter δW_{sp}.

The procedure of adjustment of the parameters B_f, $\tilde{a}_f/\tilde{a}_n$, and δW_{sp} was performed for the different variants of the phenomenological level density systematics. In the variant I we used the systematics whose parameters α, β, and γ were obtained without taking into account collective effects. In variant II we took into account collective effects at both neutron and fission channels. Moreover, for the latter we analyzed two particular cases, specifically in variant III we took $K^f_{rot}=1$, $K^n_{rot}=1$, $K^f_{vib}=1$, and $K^n_{vib}=1$, in variant IV we took into account rotational enhancement only for the fission channel ($K^n_{rot}=1$).(**) These last two variants simulate different physical situations which can take place in fission of preactinides. The variant IV corresponds to fission of spherical nuclei ($K^n_{rot}=1$) which have a higher and more sharply increasing fissility, on the contrary of the case of deformed nuclei ($K^n_{rot}=\theta_\perp T$). A similar situation may occur in the fission of a highly excited deformed nucleus. The point is that the equilibrium deformation is caused by shell effects and an excited nucleus will become spherical when shell effects disappear ($K^n_{rot}=1$). Since deformation at the saddle point has a liquid drop nature, the rotational enhancement of ρ_f will keep unchanged. Finally, the collective coefficients should have asymptotical behaviour $K_{rot}\to 1$ and $K_{vib}\to 1$ as time increases due to mixture of collective and quasiparticle degrees of freedom in a highly excited nucleus. Variant III corresponds to the case in which this phenomenon manifests at moderate excitations U≥30 MeV in both channels. Then, variant IV corresponds to the case in which suppression of collective modes "switchs on" in the fission channel later than in the neutron one (as it was predicted in ref.[47]).

The results of our analysis are presented in Table IV for preactinide nuclei whose fissility was measured as close to the fission threshold as possible. From the Table one sees that:

(i) Fission barriers heights B_f obtained on the basis of systematics of level density with collective effects (the varaints II, III, and IV) are closer to each other (discrepancies less than 1-2 MeV). The B_f values obtained on the basis of level density systematics without collective effects (the variant I) are lower of 2-3 MeV. The liquid drop barriers B_f^{LD} extracted from the empirical barriers B_f by expression (24) for variant II agree well with the results of the liquid drop model calculation[34] which is used traditionally in fission studies (see Fig. 9). The agreement between the "empirical" and calculated liquid drop fission barriers B_f^{LD} is worse for other variants. It should be remembered that for nuclides near lead (B_f-B_n≥10 MeV) there is the near threshold energy interval where the excitation energy is high for the neutron channel and one can use for the ratio Γ_f/Γ_n a Fermi-gas model description of $\rho(U)$, but at the same time the excitation energy for the fission channel is low and one must take into account correctly the pairing effects. As it was shown in ref.[45], the fission barrier

(**) As the shape of preactinide nuclides at the saddle point has the same symmetry which deformed nuclei have at the ground state, we calcualted K^f_{rot} by formula (8) with $\theta_\perp=\theta_{r.b.}f(x)$. The function f (x) of the nuclear fissility parameter x has been taken from ref.[46].

heights B_f obtained by the generalized superfluid model expressions for the nuclear level density can be different up to 2 MeV from the results of the Fermi–gas model analysis.

(ii) The largest (up to 1.16) and smallest (1.00) values of the parameter $\tilde{a}_f/\tilde{a}_n$ are provided by variant III and variant IV, respectively. The variant II has the intermediate values of the parameter $\tilde{a}_f/\tilde{a}_n$. All the values are lying within the range of different theoretical estimations, as it is shown in Fig. 10, which have a large spead.

(iii) Variants I, II, and III do not require the introduction of a noticeable shell correction δW_{sp} to describe data. This corresponds to the traditional notions about magnitude of shell effects at the fission saddle point. The small values of $\delta W_{sp} \approx -(1 \div 2)$ MeV were obtained for nuclides near lead in the variant II which are in agreement with the predictions of ref. [52]. On the contrary, the amplitude of shell effects at the saddle point is unusually large (up to $\delta W_{sp} \approx -7$ MeV) for the variant IV.

Therefore, in the analysis of data on fissility of preactinides we chose the variant II of the phenomenological systematics as the best. Moreover, for this variant it is possible to use the self-consistent description of the ground state shell corrections δW_g and the liquid drop fission barriers B_f^{LD} in the framework of the same model,[34] and reasonable values of the parameter $\tilde{a}_f/\tilde{a}_n$ and of the shell corrections at the saddle point δW_{sp}. In this variant the collective effects manifest themselves both in the neutron and fission channels. In Fig. 11 we show the results of variant II together with fissility data of different preactinide nuclei[45] as a function of excitation energy.

However, one must regard to these conclusions very carefully, especially, for what concerns the parameter $\tilde{a}_f/\tilde{a}_n$. Obviously, the preequilibrium processes and also the second chance fission after neutron emission must be taken into account when one extracts the Γ_f/Γ_n ratio from the measured fission cross-section in the high excitation energy region. As it is seen from Fig. 12, the last effect lowers the obtained Γ_f/Γ_n values. In turn, it decreases the $\tilde{a}_f/\tilde{a}_n$ value of about 0.02–0.04. The angular momentum effects work in the opposite direction. If the Γ_f/Γ_n data have been obtained by α–particle induced reactions, it may increase the $\tilde{a}_f/\tilde{a}_n$ value of about 0.02.

3.3.2 Fissility of transuranium nuclei

Unlike the case of preactinides, shell effects at the fission barrier play a decisive role for transuranium nuclei. Here the shell correction at the fission barrier is comparable with its liquid drop component. Moreover, the shell correction to the nuclear energy is an oscillating function of the deformation and this causes the double–humped shape of the fission barrier. In this case the heights of double-humped fission barrier B_f^A and B_f^B are expressed by:

$$B_f^i = \tilde{V}(\alpha_i) - \delta W_g + \delta W_{sp}^i , \qquad (25)$$

where δW^i_{sp} is the shell correction for the i–th maximum of the nuclear potential energy which is counted off the liquid drop potential energy at the corresponding deformation $\tilde{V}(\alpha_i)$.(*) The parameters of the double-humped fission barriers of transuranium nuclides have been measured in experiments with low energy particles, and compiled in ref. [54]. Some authors[53] took the values $\tilde{V}(\alpha_i)$ calculated by the liquid drop model[34] and the experimental values δW_g, B^A_f, and B^B_f, obtaining the "empirical" values for shell correction: δW^A_{sp}=2.80 MeV, and δW^B_{sp}=0.50 MeV. On this basis, the empirical fission barrier systematics for transuranium nuclei was formulated[53]. In the present paper we obtained a little different values for δW^A_{sp} and δW^B_{sp} (see Table V). We used the empirical values of the fission barrier heights B^A_f and B^B_f to calculate the fission width Γ_f. When empirical values were lacking, we derived B^A_f and B^B_f by the fission barrier systematics, although we are aware that such systematics is reliable for interpolating data, while extrapolating to the region far from the β-stability line or to the region of large Z can give uncorrect values of B^A_f and B^B_f.

The inner hump of transuranium nuclei is higher than the external one ($B^A_f > B^B_f$). The external hump height is strongly dependent on the nucleonic composition of the nucleus, in particular it decreases sharply with increasing Z. The inner hump height, on the contrary changes weakly with Z and N. As for the preactinides, the behaviour of the values of B^A_f and B^B_f of transuranium nuclei reflects the shell structure of the ground state δW_g, namely the fission barriers B_f increase approaching the subshell N= 152.

In the case of double-humped barrier the fission width is defined by the expression:[55]

$$\Gamma_f = \frac{\Gamma_A \Gamma_B}{\Gamma_A + \Gamma_B}, \qquad (26)$$

where Γ_A and Γ_B are the partial fission widths for the corresponding saddle points. Each of these widths is calculated by formula (21) with the own shell correction. The rotational enhancement coefficients K^A_{rot} and K^B_{rot} are calculated in a different way than for preactinides. Since heavy nuclei have a small deformation at the saddle point and an axially symmetric shape at the hump A, the coefficient K^A_{rot} is calculated by formula (8). This nucleus loses the mirror symmetry at the hump B and the twice larger value $K^B_{rot}=2\theta_\perp T$ corresponds to this situation.[56]

In the region of transuranium targets one extracts the ratio $\Gamma_n/\Gamma_{tot} \approx \Gamma_n/\Gamma_f$ (because $\Gamma_f \gg \Gamma_n$) from the experimental cross sections. Fig. 13 shows the experimental data on Γ_n/Γ_{tot} and their comparison with calculations. Being fission barriers of transuranium nuclides known, the experimental values B^A_f and B^B_f (or values obtained by semiempirical systematics for fission barriers) and also the "empirical" values of the shell corrections δW^A_{sp} and δW^B_{sp} have been used in the calculation of Γ_f. The $\tilde{a}_f/\tilde{a}_n$ parameter were adjusted to reproduce the experimental data. As transuranium nuclei have a relatively large deformation in the ground state and their deformation at the saddle point do not differ strongly from the equilibrium deformation, the Γ_n/Γ_f ratio will not be so sensitive to collective effects as in the

(*) The deformations of transuranium nuclides $\alpha_A \approx 0.3$, $\alpha_B \approx 0.6$ are slightly dependent on the nucleonic composition.[53]

case of preactinides. Therefore, we show only the results of calculations with level density systematics parameters α, β, and γ obtained by taking into account collective effects (solid line curve in Fig.13).

A high sensitivity of fissility to shell effects is a peculiarity of transuranium nuclei. To select the shell effects influence we performed also the calculation without shell effects for each case. As it is seen from Fig. 13 (dashed-line curve), the shell effects are fastly destroyed with increasing of the excitation energy, disappearing at $U \geq 30$ MeV while at low excitations, $U \leq 20$ MeV, they prevent the fission.

Fig. 14 illustrates the sensitivity of the Γ_n/Γ_{tot} ratio to the value of the shell corrections at the neutron channel δW_n and at the saddle point δW_{sp}^A for the ^{256}Md nuclide. (As the external hump is small, the fissility of transfermium nuclei is determined mainly by the inner hump). The variation of δW_n or δW_{sp}^A of only 1 MeV changes the Γ_n/Γ_{tot} ratio approximately by a factor of 2. So the availability of more correct data on the fissility of transfermium nuclei would allow to obtain more reliable information about shell corrections at the ground state and at the saddle point and about velocity of damping of shell effects in heated nuclei.

3.4 Time lives of excited nuclei

We analyzed experimental data on time lives of compound nuclei with $5 \leq U < 15$ MeV produced in nuclear reactions initiated by low energy neutrons, protons and α-particles. Time lives of medium weight (A~110) compound nuclei produced in (p,p') reaction were measured by X–ray spectroscopy,[57,58] and time lives of heavy (A~240) compound nuclei produced in (n,xnf), (p,xnf), (α,xnf) reactions were measured using the crystal-blocking technique.[59–62] In this case the evaporation chain is short (x =1 or 2), and consequently it is possible to select the decay of different excited nuclei in the evaporation chain by analyzing the first and second chance fission. We extracted from these data the absolute value of the total decay width $\Gamma_{tot} \equiv \sum_j \Gamma_j$ by the expression:

$$\tau = \hbar / \Gamma_{tot} . \qquad (27)$$

We did not consider data obtained in heavy ion reactions, because, in this case, the excitation energy of compound nucleus is high, the evaporation chain is long, and the interpretation of the process is more complicated due to the high angular momentum of compound nucleus. So such experiments give only an effective time life which can not be put in correspondence to the actual nucleus with given value of excitation energy.[59] Moreover, from the theoretical point of view it is also a serious problem to analyze time lives of highly excited nuclei. In fact, the expression (27) is valid only for decay of an isolated level, while a highly excited nucleus has strongly overlapping levels and, due to their interference, time life will exceed significantly the estimated value (27) for the case of an isolated level.[63]

The time life (deduced from the total decay width) is more sensitive to the nuclear level density than the nuclear fissility (deduced from the ratio Γ_f/Γ_{tot}). Moreover, usually one or two channels dominate the nuclear decay. Then it is possible to determine the given partial width from the measured time life. For example, in the case of medium weight nuclei (like ^{107}In and ^{113}Sb), the main decay channel is the neutron emission and, in the case of heavy nuclei (like ^{239}U, ^{239}Np, ^{238}Pu, and ^{239}Pu), these channels are the neutron and the fission ones.

Fig. 15 shows data on time lives and their comparison with calculations. Both calculation based on M-S[34] and C[35] shell corrections give similar results. The calculation which takes into account collective effects (curves 1) gives time lives values which are considerably lower than the calculation without collective effects (curves 2). The partial widths are strongly influenced by collective effects in spite of the fact that they depend on the ratio of level densities of compound and residual nuclei, and so collective enhancement of level density is partially compensated. The quality of data is not good enough to draw definite conclusions. However, on the whole the calculation with collective effects describes the experiment better than the calculation without collective effects. The calculated time lives drop with energy faster than the experimental ones. It would be desirable to measure correctly time lives of different nuclides in the energy region 10<U<15 MeV to investigate this discrepancy. There is also a discrepancy in the region of low energies caused by the fact that the residual nucleus in the neutron or fission channels has a very low excitation energy ($U-B_n$) or ($U-B_f$). As it was mentioned, one must take into account pairing effect in a more correct manner and use relationships of the generalised superfluid model.[45] Moreover, in the case of low excited heavy nuclei one ought to use, instead of eq. (26), a more correct expression for Γ_f which takes into account the population of the states of the second potential well and the non-radiative transitions through the inner barrier of the double-humped fission barrier.[61]Using such correct expression for Γ_f and also varying the pairing parameters in the neutron, Δ_n, and fission, Δ_f, channels it would be possible to descibe the dependence $\tau(U)$ in the low energy region, U~(6÷7) MeV. But a correct description of the nuclear level density at low energy region was not in the aim of the present paper.

4. CONCLUSION

In the present paper the total bulk of data on level density, decay widths and time lives of excited compound nuclei has been analyzed in the framework of the statistical approach. The phenomenological level density systematics,[11] based on the Fermi-gas model relationships and taking into account the shell and collective effects, is able to describe the absolute values of level density for different nuclides in the energy range from ~5 MeV to ~ 20 MeV with accuracy of a factor 2. The same accuracy has been achieved in the description of data on radiative width Γ_γ. An analysis of data on compound nucleus fissilities allowed us to widen the excitation energy region under study and to get an information about the level density of nuclei with high deformation (at the fission saddle point). Moreover, fissility of preactinide nuclei is most sensitive to the collective effects at the level density, and fissility of transuranium nuclei is most sensitive to the shell effects.

It follows from the analysis of existing data that: *(i)* shell effects manifest themselves most strongly in the level density and partial decay widths of cold nuclei and they disappears at energies U>30 MeV; and *(ii)* collective effects are suppressed slowerly and must be taken into account, at least up to excitations U≈(30÷50) MeV, in both emission and fission channels.

Taking into account collective effects, it is possible to improve the agreement with experiment and also to get reasonable asymptotical Fermi-gas values of the level density parameter which are not in contradiction with the data on evaporation spectra. To obtain a further better accuracy, one needs to take into account the rotational enhancement of the nuclear level density even for nuclei which have a small deformation.

The obtained accuracy of the simple phenomenological expressions allowed the formulation of a reliable evaporation model for describing the decay of nuclei which have the excitation energy $B_n \leq U \leq 100$ MeV. The parameters of this model have been fixed by analyzing the totality of independent experimental data. To get higher reliance of the evaporation model at high excitation energy region one needs to solve the problems connected with suppression of collective states contributions to level density at high excitation energy[45] and with temperature dependence of the asymptotic level density parameter $\tilde{a}$ caused by the effects of nuclear medium on the nucleon mass (the variation with temperature of the effective mass).[64]

The authors are deeply indebted to G.D. Adeev, E.A. Cherepanov, T. Von Egidy, A.V. Ignatyuk, M.V. Kazarnovsky, V.M. Lobashev, V.V. Pashkevich, S.Shlomo, and G.N. Smirenkin for interesting and stimulating discussions.

Two of us (ASİ and MVM) express their gratitude to the INFN for its hospitality during their stay at the Frascati National Laboratories.

REFERENCES

1. V.S. Barashenkov, A.S. Iljinov, N.M. Sobolevsky, V.D. Toneev.Usp. (Sov. Phys.), 109, 91 (1973); A. S. Iljinov, V.I. Nazaruk, S.E. Chigrinov. Nucl. Phys., A 268, 513 (1976), Nucl. Phys., A382, 378 (1982); A.S. Iljinov, M.V. Mebel, C. Guaraldo, V. Lucherini, E. De Sanctis, N. Bianchi, P. Levi Sandri, V. Muccifora, E. Polli, A.R. Reolon, P. Rossi. Phys. Rev., 39C, 1420 (1989).
2. T. Ericson. Adv. in Phys., 9, 425 (1960).
3. J.R. Huizenga, L.G. Moretto. Ann. Rev. Nucl. Sci., 22, 472 (1972).
4. A.V. Ignatyuk. The Statistical Properties of the Excited Atomic Nuclei. Energoatomizdat, Moscow, 1983.
5. A. Gilbert, A.G. W. Cameron. Can J.Phys., 43, 1466 (1965); P.J. Brancazio, A.G. W. Cameron. Can. J. Phys., 47, 1029 (1967).
6. T.D. Newton. Can J. Phys. 34, 804 (1956).
7. W. Dilg, W. Schantl, H. Vonach, M. Uhl. Nucl. Phys., A217, 269 (1973).

8. T.von Egidy, H.M. Schmidt, A.N. Bekhami. Nucl. Phys., A 481, 189 (1988).
9. P. Decowski, W. Grochulski, A. Marcinkowski, K.Siwek, Z. Wilhelmi. Nucl. Phys., A 110, 129 (1968).
10. A.V. Ignatyuk, Yu.N. Shubin. Yad. Fiz. 8, 1135 (1968).
11. A.V. Ignatyuk, G.N. Smirenkin, A.S. Tishin. Yad. Fiz. 21, 485 (1975).
12. K.H. Schmidt, H. Delagrange, J.P. Dufour, N. Carjan, A. Fleury. Z. Phys, A308, 215 (1982).
13. A.S. Iljinov, E.A. Cherepanov. Nukleonika, 25, 611 (1980); Preprint INR AS USSR P-0064, Moscow, 1977.
14. J.Töke, W. J. Swiatecki. Nucl. Phys. A372, 141 (1981).
15. S. Bjørnholm, A. Bohr, B. Mottelson. Proc. of the Symp. on Phys. and Chem. of Fission, v. 1, IAEA, Vienna, 1974,p. 367.
16. M. Hagelund, A.S. Jensen. Phys. Scr. 15, 225 (1977).
17. A.H. Wapstra, G. Audi. Nucl. Phys. A432, 55 (1985).
18. S.F. Mughabghab, M. Divadeenam, N.E. Holden. Neutron cross sections, vol. 1, part A (Academic Press, N.Y., 1981);
    S.F. Mughabghab. Neutron cross sections, vol.1, part B (Academic Press, N.Y., 1984).
19. G.Rohr, L. Maissano, R. Shelly. Proc. of the specialists meeting on neutron cross sections of fission product nuclei, Bologna, 1979, p.197.
20. T.S. Belanova, A.V. Ignatyuk, A.B. Paschenko, V.E. Plyaskin. Neutron radiative capture, Handbook. Energoatomizdat, Moscow, 1986.
21. A.V. Malyshev. Level Density and Structure of Atomic Nuclei. Atomizdat, Moscow, 1969.
22. E. Erba, U. Facchini, E. Saetta–Menicella. Nuovo Cim. 22, 1237 (1961).
23. J.E. Lynn. The theory of neutron resonance reactions. Clarendom Press, Oxford, England, 1968.
24. H.Baba. Nucl. Phys. A 159, 625 (1970).
25. S.F. Mughabghab, D.I. Garber. Neutron cross sections. BNL – 325, 3rd ed., vol.1 (1973).
26. D.Kopsch, S. Cierjacks. Statistical properties of nuclei. Plenum Press, NY–London (1972), p.455.
27. J.R. Huizenga, H.K. Vonach, A.A. Katsanos, A.J. Gorski, C.J. Stephan. Phys. Rev. 182, 1149 (1969).
28. A.A.Katsanos, R.W.Shaw, R.Vandenbosch, D.Chamberlin, Phys. Rev., 1C, 594 (1970).
30. C.C. Lu, L.C. Vaz, J.R. Huizenga. Nucl. Phys. A 190, 229 (1972).
31. M. Hillman, J.R. Grover. Phys. Rev., 185, 1303 (1969).
32. H.R. Groening, W.D. Loveland. Phys. Rev., 10C, 697 (1974).
33. M. Beckerman. Nucl. Phys., A278, 333 (1977).
34. W.D. Myers, W.J. Swiatecki. Ark. Fysik, 36, 343 (1967).
35. J.W. Truran, A.G. W. Cameron, E. Hilf. Proc. Int. Conf. on the Properties of Nuclei, Leisin, 1970, vol. 1, p. 275.
36. R.W.Hasse, P. Schuck. Phys. Lett. 179B, 313 (1986).
37. A. Chbini, L.G. Subotka, N.G. Nicolis, D. G. Sarantites, D.W. Stracener, Z. Majka, D.C. Hensley, J.R. Beene, M. L. Halbert. Phys. Rev.43C, 666 (1991).

38. P. Möller, J. R. Nix. Preprint LA–UR–86–3983, Los Alamos, 1986.
39. L.G. Moretto. Proc. 3rd IAEA Symp. on the Phys. and Chem. of Fission, Rochester (Vienna, IAEA), 1973.
40. A.S. Iljinov, E.A. Cherepanov, Yu. Ts. Oganessian. Yad. Fiz. 33, 997 (1981).
41. E.A. Cherepanov, A.S. Iljinov, M.V. Mebel. J. Phys. G: Nucl. Phys. 9, 1397 (1983).
42. I. Dostrovsky, Z. Fraenkel, G. Friedlander. Phys. Rev., 116, 683 (1959).
43. G. Reffo. IAEA Second Panel on Fission Product Nuclear Data, Petten, 5–9 September, 1977.
44. H. Malecki, A.B. Popov, K. Tshezak. Sov. J. Nucl. Phys., 37, 169 (1983); JINR Preperint P3 –82–11, Dubna, 1982.
45. A.V. Ignatyuk, G.N. Smirenkin, M.G. Itkis, S. I. Mulgin, V.N. Okolovich. Sov. J. Part. Nucl., 16, 307 (1985).
46. V.M. Strutinsky. Yad. Fiz., 1, 821 (1965).
47. G. Hansen, A.S. Jensen. IAEA Advisory Group Mecting on Basic and Applied Problems of Nuclear Level Densities, Upton, 1983. Rep. BN–NCS–51694, p. 161.
48. A.V. Ignatyuk, M.G. Itkis, V.N. Okolovich et al. Yad. Fiz., 21, 1185 (1975) [Sov. J. Nucl. Phys., 21, 612 (1975)].
49. W. Reisdorf. Z. Phys., A 300, 272 (1981).
50. J. Treiner. IAEA Advisory Group Meeting on Basic and Applied Problems of Nuclear Level Densities, Upton, 1983. Rep. BNL–NCS–51694, p.383.
51. E.M. Rastopchin, Yu. B. Ostapenko, M.I. Svirin, G.N. Smirenkin. Yad. Fiz., 49, 24 (1989) [Sov. J. Nucl. Phys., 49, 15 (1989)].
52. U. Mosel. Phys. Rev., 6C, 971 (1972).
53. V.M. Kupriyanov, K.K. Istekov, B.I. Fursov, G.N. Smirenkin,Yad. Fiz., 32, 355 (1980).
54. M. Dahlinger, D. Vermeulen, K.–H. Schmidt. Nucl. Phys., A376, 94 (1982).
55. V.M. Strutinsky, S. Bjørnholm. Int. Symp. on Nucl. Structure, Dubna (Vienna: IAEA), vol. 1 p. 409.
56. P. Möller, J.R. Nix, Proc. 3rd IAEA Symp. on the Phys. and Chem. of Fission, Rochester (Vienna: IAEA), vol. 1, p. 103.
57. S. Röhl, S. Hoppenau, M. Dost. Phys. Rev. Lett. 43, 1300 (1979).
58. J.F. Chemin, S.Andriamonje, J. Roturier, B. Saboya, J.P. Thibaud, S. Joly, S. Plattard, J. Uzureau, M. Laurent, J.M. Maison, J.P. Shapira.Nucl. Phys., A331, 407 (1979).
59. J.U. Anderson, K.O. Nielsen, J. Skak-Nielsen, R. Hellborg, K.G. Prasad. Nucl. Phys., A 241, 317 (1975); A 324, 39 (1979).
60. Yu. V. Melikov, Yu. D. Otstavnov, A.F. Tulinov, N.G. Chetchenin. Nucl. Phys. A 180, 241 (1972).
61. V.O. Kordjukevich, Yu. V. Melikov, S. Yu. Platonov, A.F. Tulinov, O.V. Fotina, O.A. Yuminov. Nucl. Phys. A492, 447 (1989).
62. A.V. Grusha, V.O. Kordjukevich, Yu. V. Melikov, L.N. Syutkina, A.F. Tulinov, O.A. Yuminov. Nucl. Phys. A429, 313 (1984).
63. V.L. Lyuboshits. Sov. J. Nucl. Phys. 27, 502 (1978); 37, 174 (1983).
64. S.Shlomo, J.B. Natowitz. Phys. Lett. 252B, 187 (1990).

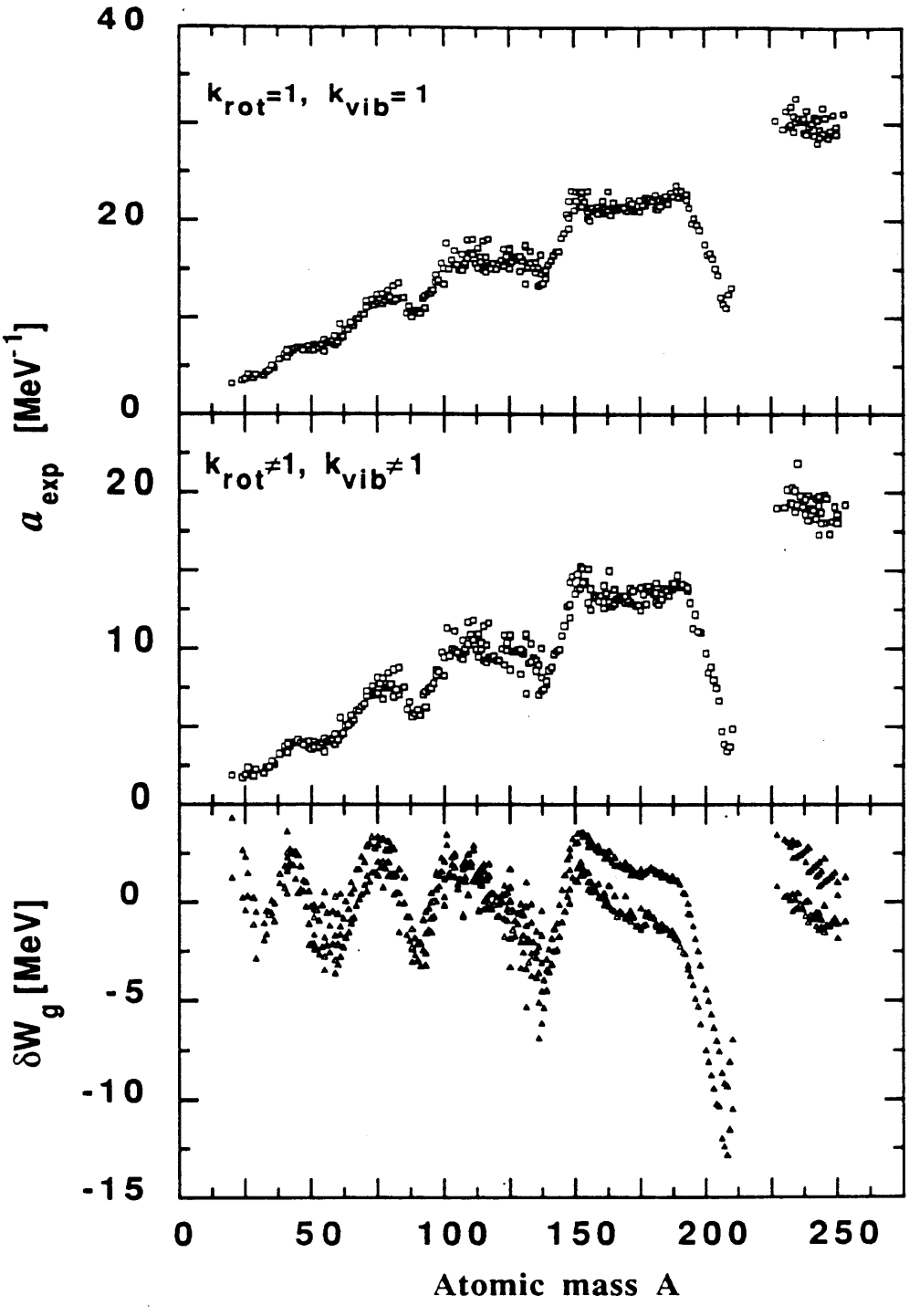

FIG. 1 - Experimental values of the level density parameter a_{exp} and the empirical ground state shell correction δW_g as a function of the atomic mass A. The a_{exp} values extracted without (K_{rot}=1,and K_{vib}=1) and with ($K_{rot}\neq 1$, and $K_{vib}\neq 1$) collective effects are shown. The shell corrections are determined on the basis of M-S (open triangles) and C (full triangles) liquid drop model parameters.

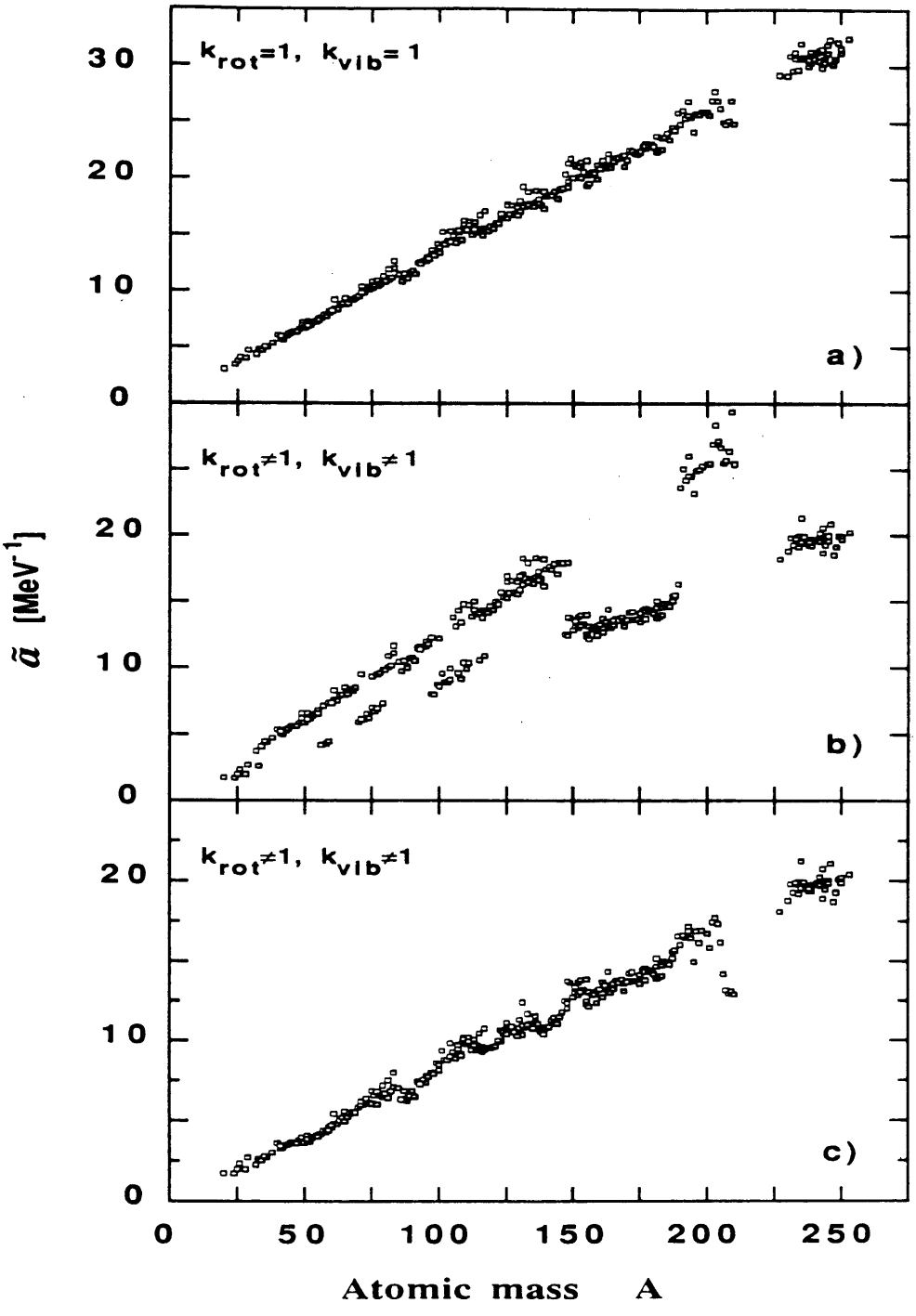

FIG. 2 - A–dependence of the asymptotic value of the level density parameter $\tilde{a}$. extracted without ($K_{rot}=1$, and $K_{vib}=1$) [Fig.a] and with ($K_{rot}\neq1$, and $K_{vib}\neq1$) collective effects. For the latter, two cases are shown: respectively, when nuclei with deformation $\beta>0.17$ [Fig.b] and $\beta\geq0$ [Fig.c] are assumed to be deformed.

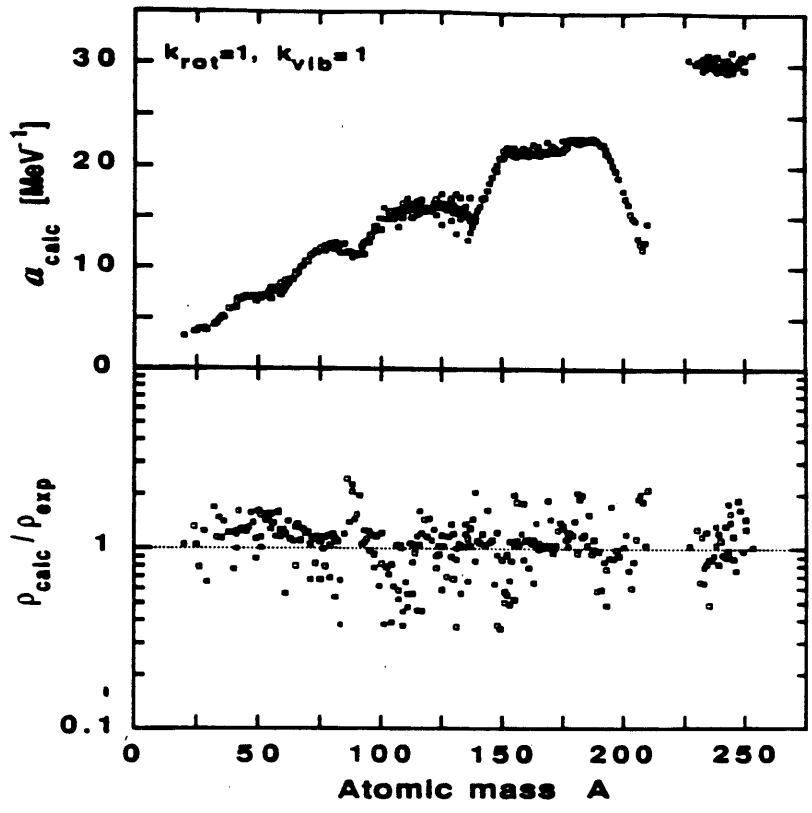

FIG. 3 - A-dependence of the theoretical level density parameter a_{calc} and the ratio ρ_{calc}/ρ_{exp} for the phenomenological level density systematics without taking into account collective effects, and with M-S shell corrections.

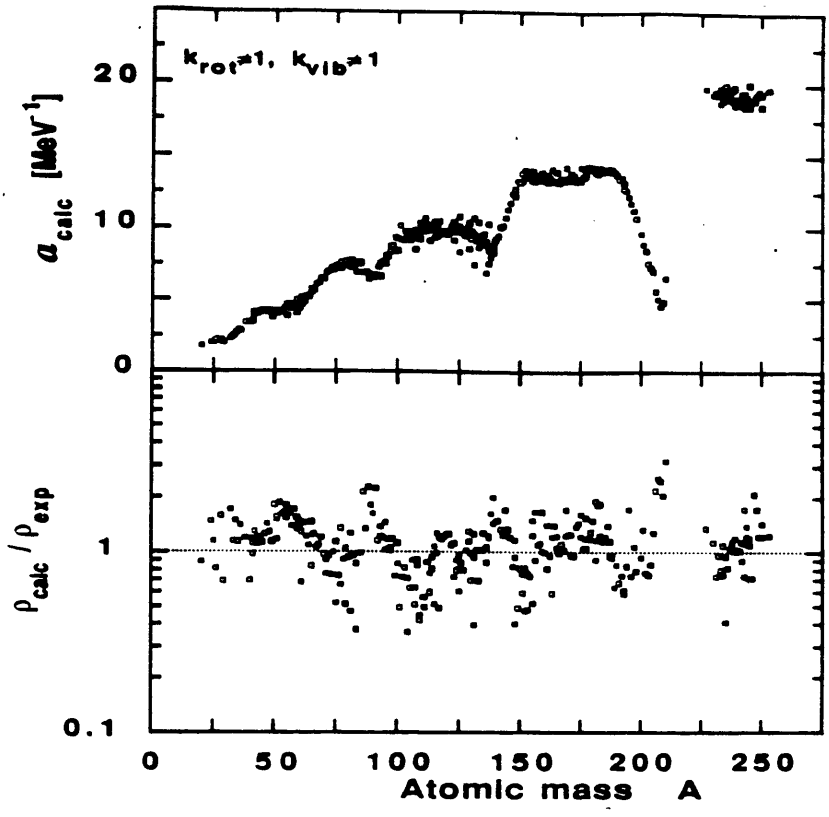

FIG. 4 - The same as Fig. 3 but for the phenomenological level density systematics taking into account collective effects.

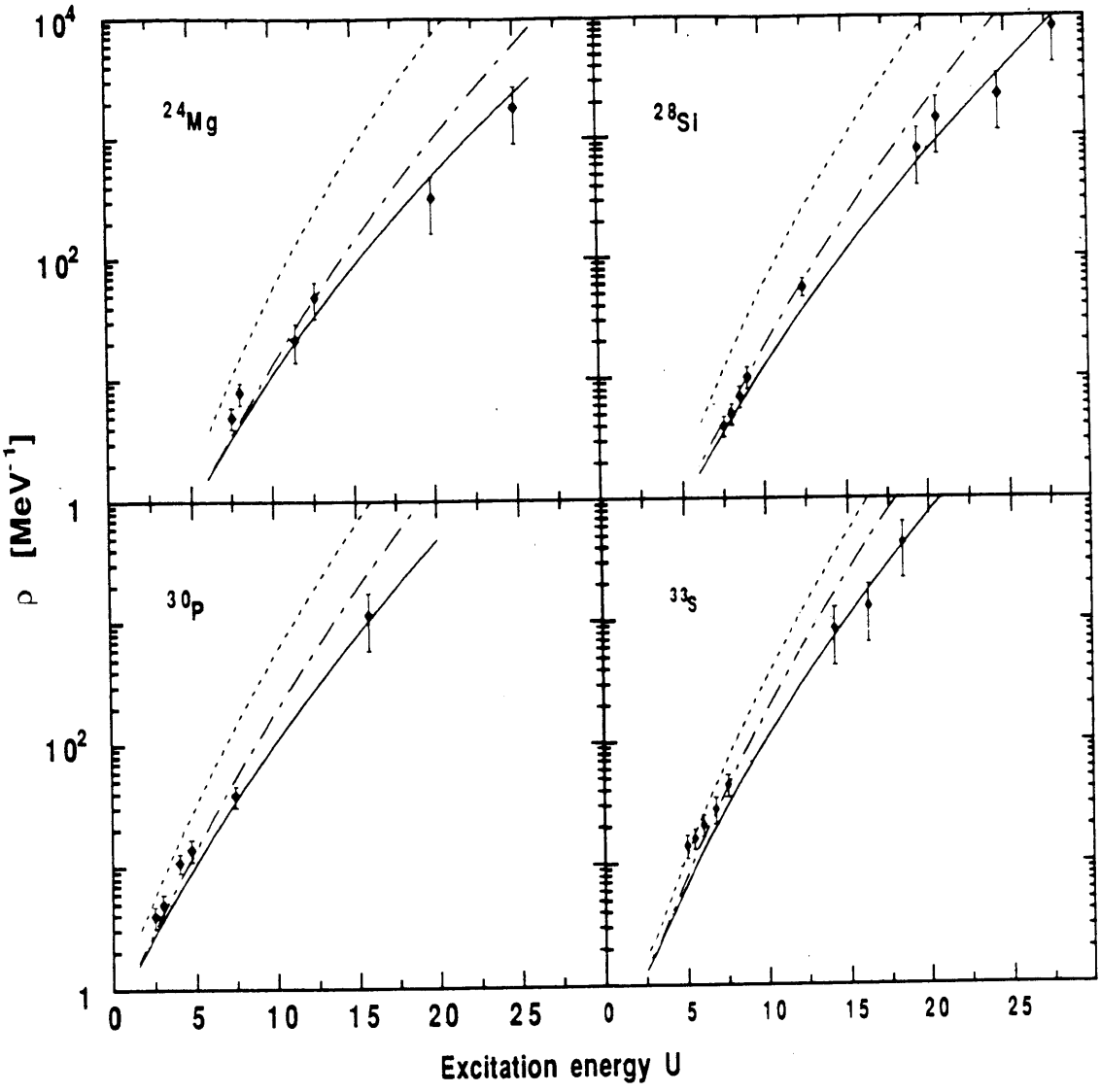

FIG. 5 - Energy dependence of the level densities of nuclides ^{24}Mg, ^{28}Si, ^{30}P, and ^{33}S. Points are the experimental data given in Table II. The solid and dot-dashed curves are the results of calculation with and without collective effects, respectively, and with the M-S shell corrections. The dashed curves are the calculation results without collective effects and with C shell corrections.

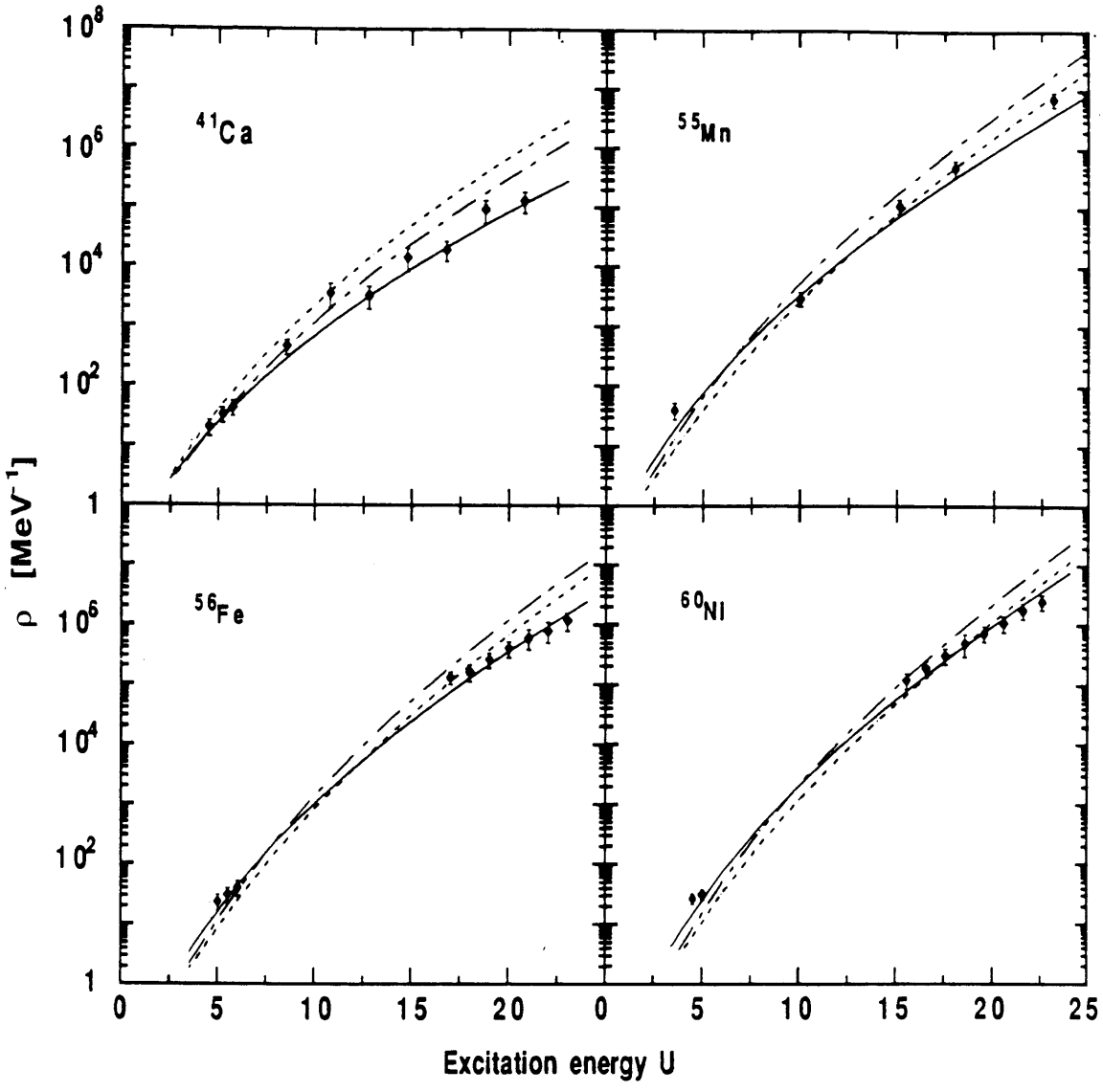

FIG. 6 - The same as fig. 5 for ^{41}Ca, ^{55}Mn, ^{56}Fe, and ^{60}Ni nuclides.

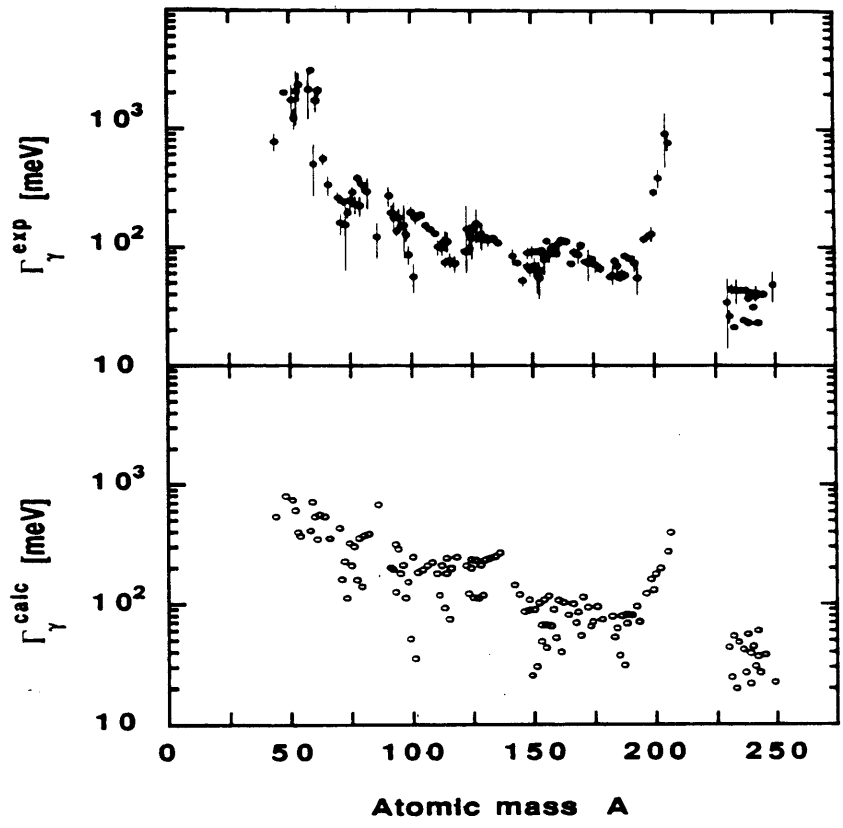

FIG. 7 - A-dependence of the neutron resonance radiative width Γ_γ. Experimental points are taken from ref. [44]. The calculation was performed with M-S shell corrections and with collective effects.

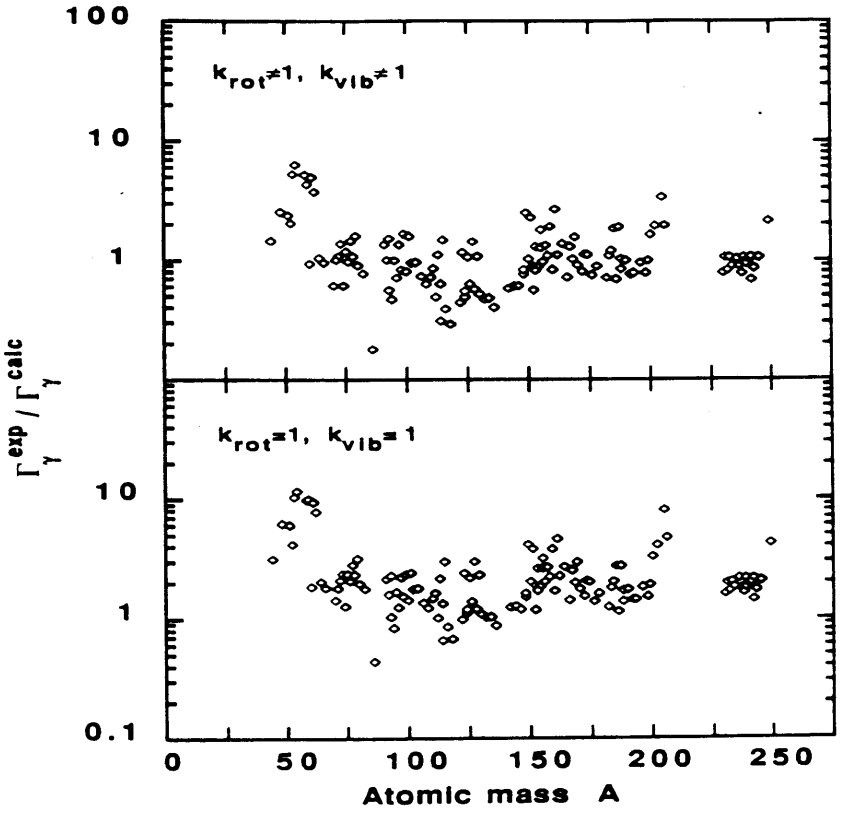

FIG. 8 - A-dependence of $\Gamma_\gamma^{exp}/\Gamma_\gamma^{calc}$ ratio for the calculations with ($K_{rot}\neq1$, and $K_{vib}\neq1$) and without ($K_{rot}=1$, and $K_{vib}=1$) collective effects, both with the M-S shell corrections.

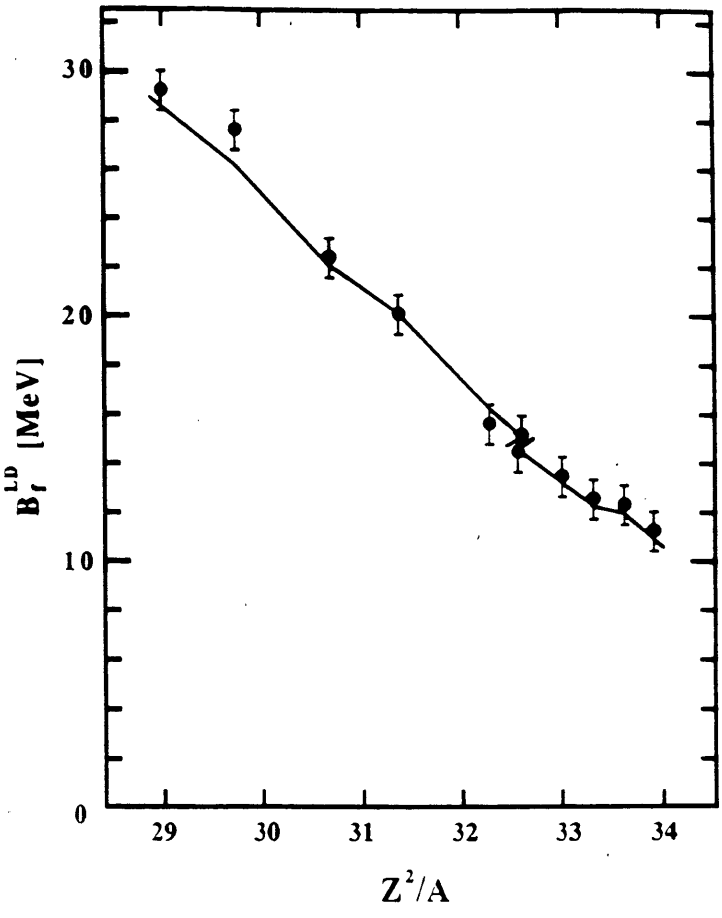

FIG. 9 - Dependence of the liquid drop fission barrier heights B_f^{LD} on the parameter Z^2/A. The points are B_f^{LD} values extracted from the analysis of the nuclear fissilities. The curve is the liquid drop model[34] calculation results.

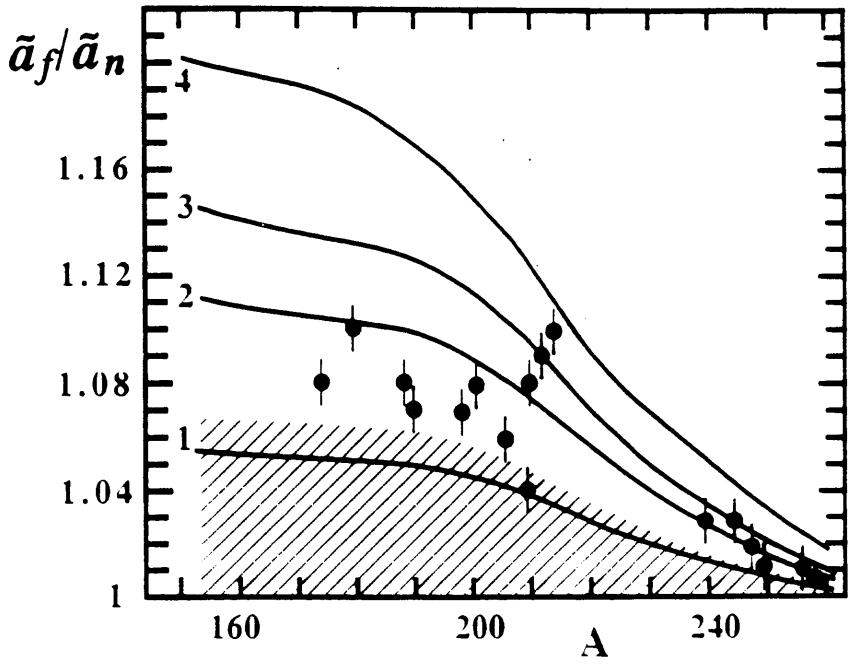

FIG. 10 - A-dependence of the $\tilde{a}_f/\tilde{a}_n$ ratio. The curves are the results of theoretical estimations: curve 1, ref. [48]; curve 2, ref. [49]; curve 3, ref. [14], curve 4, ref. [50]. The shaded area represents the results of the analysis of nuclear fissilities performed in ref. [51]. The points are results of our analysis.

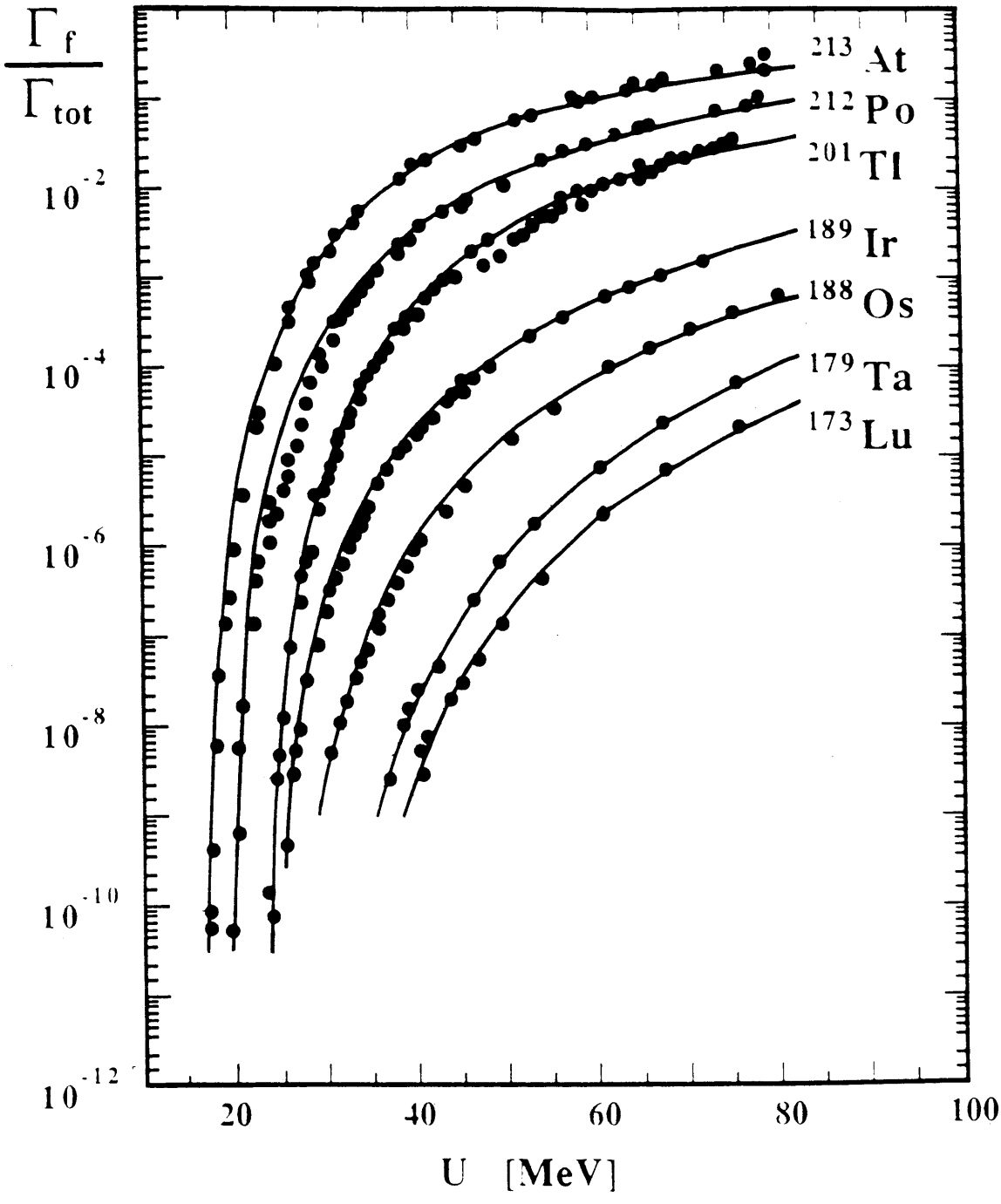

FIG. 11 - Excitation energy dependence of the fissility Γ_f/Γ_{tot} of different compound nuclei. Curves are the calculation results with M-S shell corrections and with collective effects. Experimental points were taken from ref.[45].

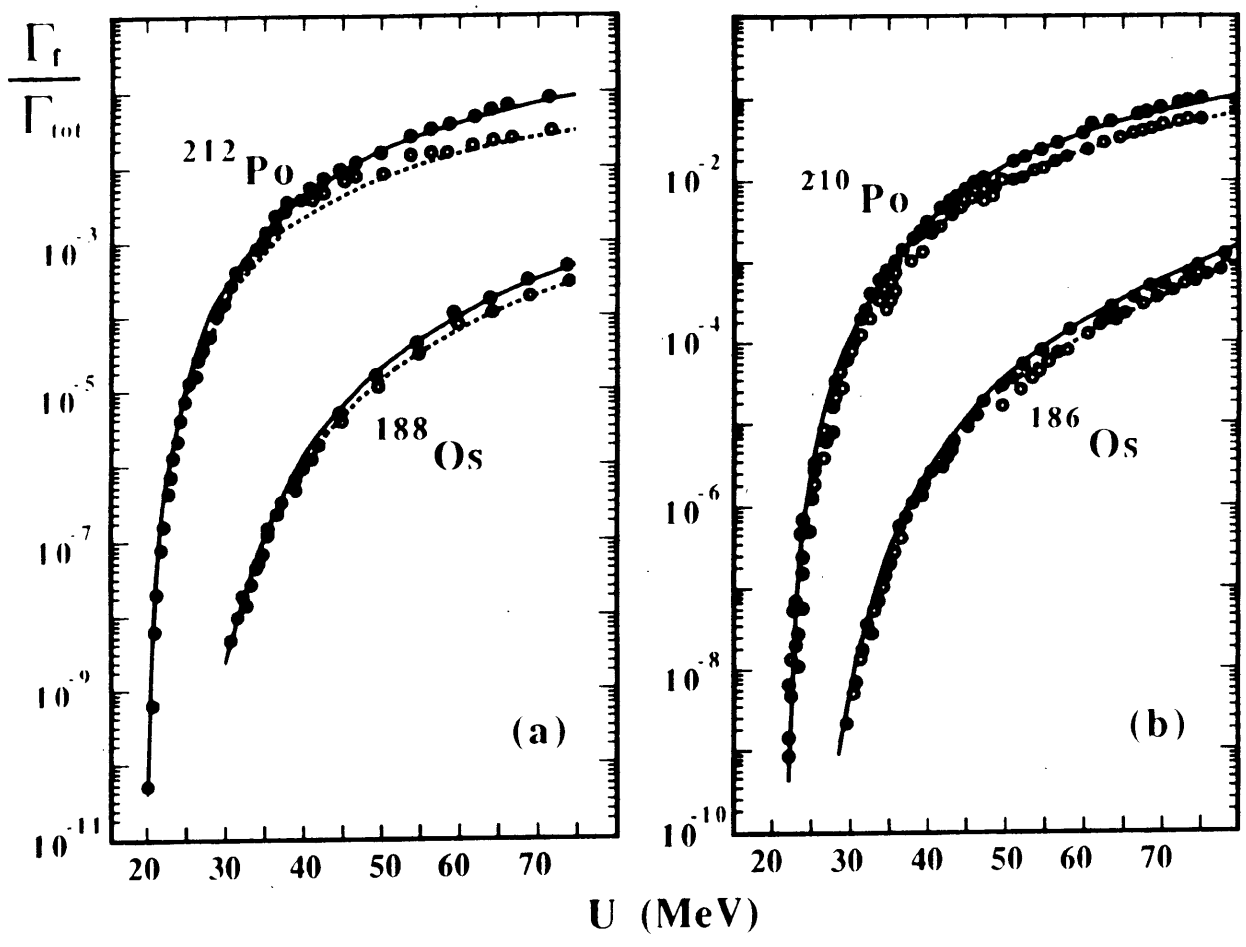

FIG. 12 - First chance fission and angular momentum effects on nuclear fissility. Fig. (a): full circles are the observed fissility values, the open circles are the "first chance" fissility[45]. The solid curves are the calculation results with $\tilde{a}_f/\tilde{a}_n$=1.09 (^{212}Po) and $\tilde{a}_f/\tilde{a}_n$=1.08 (^{188}Os). The dashed curves are the calculation results with $\tilde{a}_f/\tilde{a}_n$=1.05 (^{212}Po) and $\tilde{a}_f/\tilde{a}_n$=1.06 (^{188}Os).
Fig. (b): full and open circles are the fissilities of nuclei by α–particles and protons respectively.The solid curves are the results of calculation with $\tilde{a}_f/\tilde{a}_n$=1.09 (^{210}Po) and 1.11 (^{186}Os). The dashed curves are the results of calculation with $\tilde{a}_f/\tilde{a}_n$=1.07 (^{210}Po) and 1.09 (^{186}Os).

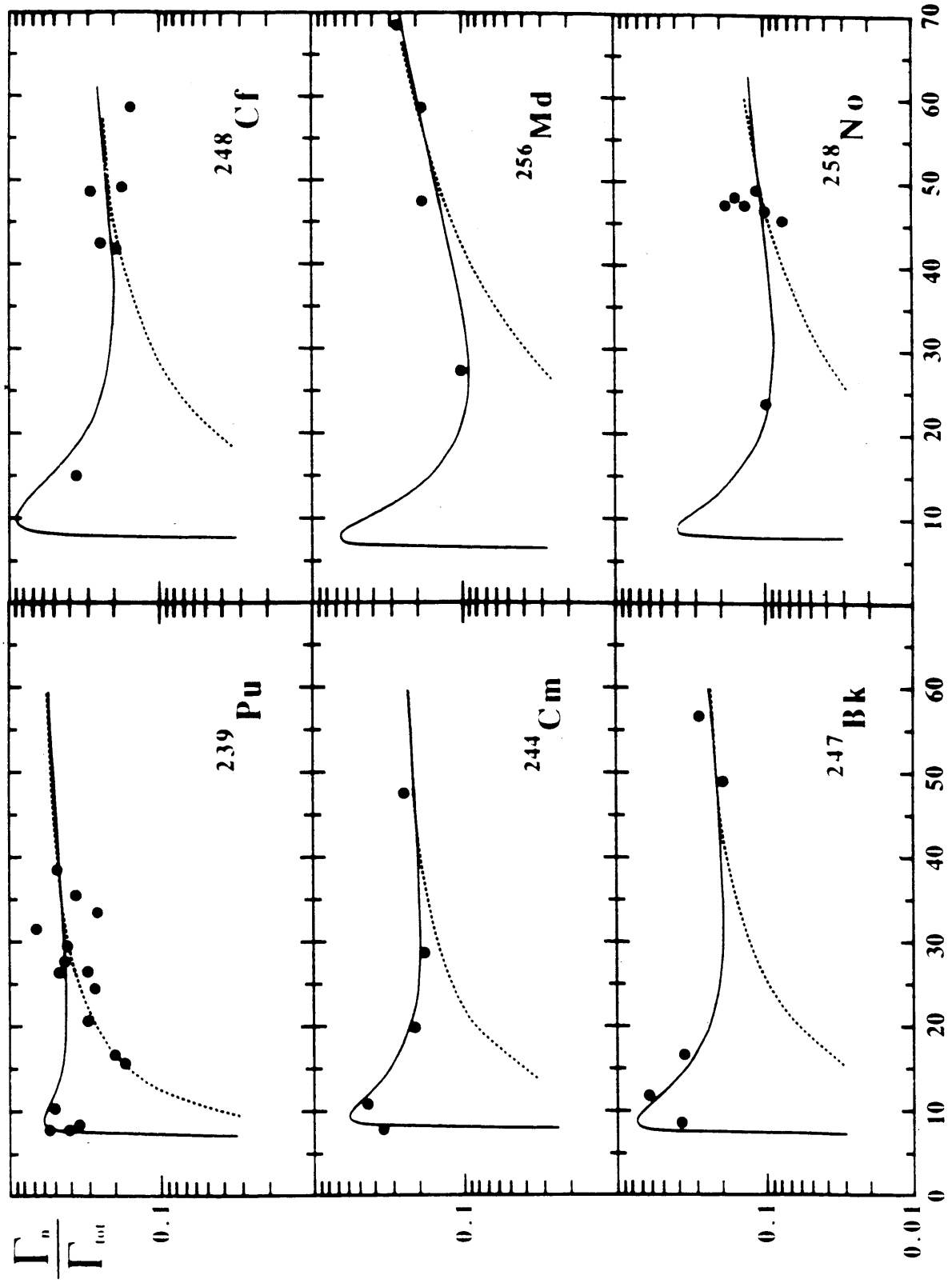

FIG. 13 - Energy dependence of the neutron emission probability Γ_n/Γ_{tot} for transuranium nuclei. The experimental points were taken from ref.[41]. The full curves are the calculation with collective effects and with M-S shell corrections, the dashed curves are the calculation without shell effects.

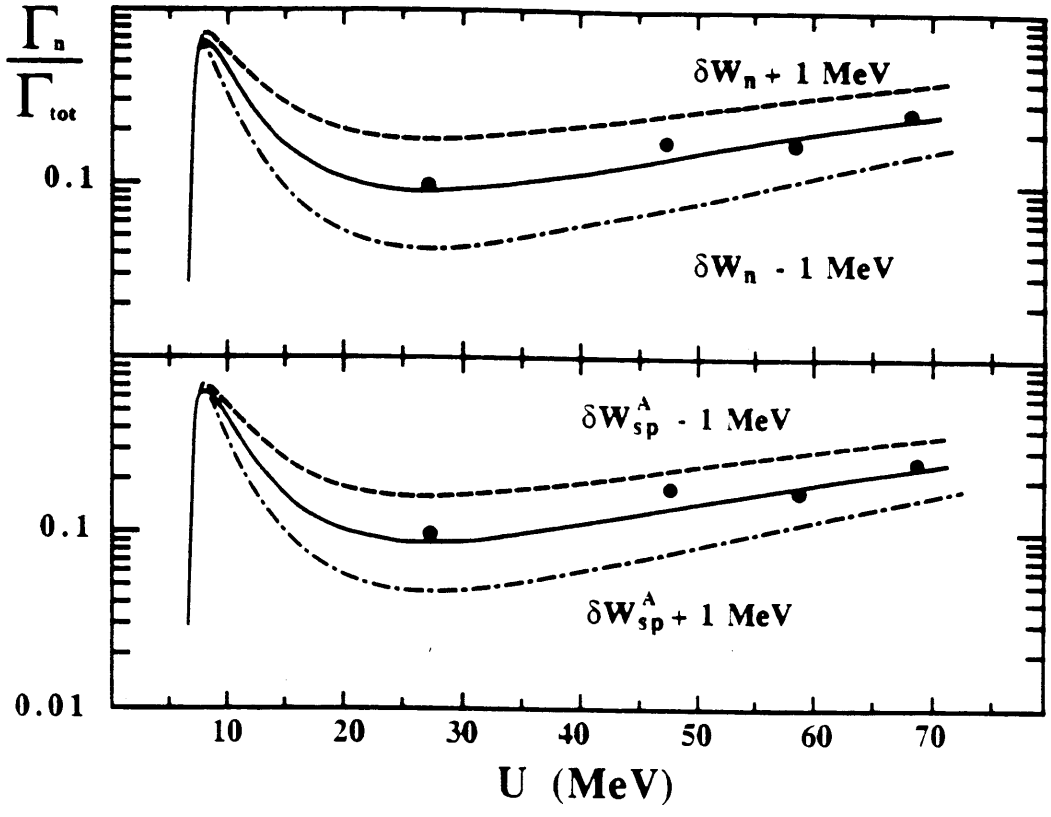

FIG. 14 - Energy dependence of the Γ_n/Γ_{tot} ratio for ^{256}Md. Full curve is as in Fig. 13. Upper part: dashed and dott–dashed curves are the calculations with the neutron channel shell correction 1 MeV larger, and smaller, respectively.
Lower part: dashed and dott–dashed curves are the calculations with the saddle point shell correction 1 MeV smaller and larger , respectively.

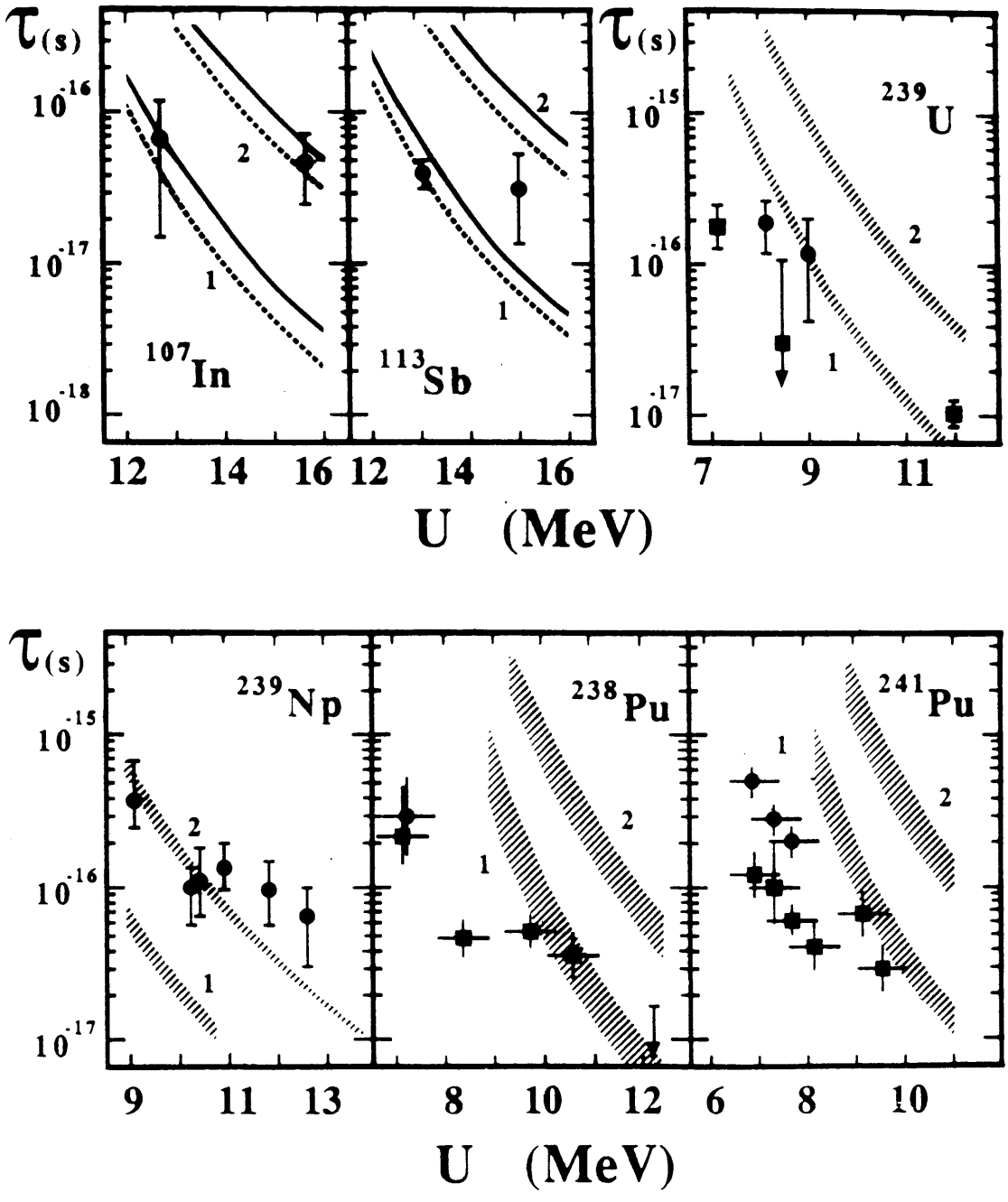

FIG. 15 - The time-lives τ of different nuclei as a function of the excitation energy U. Experimental points are from refs. [58] (^{107}In), [57] (^{113}Sb), [59,60] (^{239}U), [61] (^{239}Np), [62] (^{238}Pu, ^{241}Pu). Curves 1 and 2 refer to the calculation with and without collective effects, respectively. The solid line curves are the calculation with M-S shell corrections, the dashed curves are the calcualtion with C shell corrections. The shaded area corresponds to the uncertainties of the experimental parameters of double–humped fission barriers.

TABLE I - Neutron resonance data on nuclear level density.

Nuclide	Spin	B_n (MeV)	D (eV)	ΔD (eV)	a_{exp} (MeV $^{-1}$) I	II	Ref.
^{20}F	0.5	6.601	1.60E+05	4.00E+04	3.22	1.87	(19)
^{24}Na	1.5	6.959	9.50E+04	3.00E+04	3.49	1.75	(19)
^{25}Mg	0.0	7.331	4.70E+05	1.40E+05	3.67	1.92	(19)
^{26}Mg	2.5	11.093	5.50E+04	1.70E+04	4.16	2.37	(19)
^{28}Al	2.5	7.725	5.50E+04	1.50E+04	3.83	1.85	(21)
^{29}Si	0.0	8.474	2.00E+05	6.00E+04	4.09	2.29	(19)
^{32}P	0.5	7.937	7.50E+04	2.00E+04	3.99	2.02	(19)
^{34}S	1.5	11.417	2.70E+04	1.00E+04	4.57	2.44	(19)
^{35}S	0.0	6.986	2.00E+05	7.00E+04	5.04	2.81	(19)
^{33}S	0.0	8.642	1.50E+05	3.50E+04	4.42	2.39	(19)
^{36}Cl	1.5	8.580	1.30E+04	4.00E+03	4.82	2.60	(24)
^{38}Cl	1.5	6.108	2.10E+04	6.50E+03	5.70	3.26	(19)
^{41}Ar	0.0	6.099	9.50E+04	2.40E+04	6.71	4.03	(19)
^{40}K	1.5	7.800	4.30E+03	5.00E+02	6.20	3.75	(24)
^{41}K	4.0	10.096	2.50E+03	2.50E+02	6.56	3.89	(19)
^{42}K	1.5	7.534	4.80E+03	1.20E+03	6.34	3.78	(24)
^{41}Ca	0.0	8.363	4.50E+04	1.00E+04	5.85	3.35	(18)
^{43}Ca	0.0	7.933	2.80E+04	5.00E+03	6.63	3.98	(19)
^{44}Ca	3.5	11.132	2.60E+03	4.00E+02	6.81	4.00	(19)
^{45}Ca	0.0	7.415	3.30E+04	6.00E+03	6.92	4.14	(19)
^{49}Ca	0.0	5.147	2.60E+05	9.00E+04	6.79	3.63	(24)
^{46}Sc	3.5	8.761	1.30E+03	1.00E+02	6.86	3.99	(18)
^{47}Ti	0.0	8.878	1.69E+04	2.50E+03	6.63	3.84	(19)
^{48}Ti	2.5	11.627	1.60E+03	4.00E+02	6.86	3.99	(19)
^{49}Ti	0.0	8.143	2.00E+04	3.20E+03	7.03	4.08	(19)
^{50}Ti	3.5	10.939	3.60E+03	9.00E+02	6.62	3.58	(19)
^{51}Ti	0.0	6.372	7.10E+04	4.00E+04	7.21	4.04	(19)
^{51}V	6.0	11.051	1.40E+03	3.00E+02	7.01	3.78	(19)
^{52}V	3.5	7.311	4.39E+03	5.30E+02	6.84	3.64	(20)
^{51}Cr	0.0	9.262	1.50E+04	2.00E+03	6.65	3.69	(18)
^{53}Cr	0.0	7.940	2.90E+04	5.00E+03	6.96	3.82	(19)
^{54}Cr	1.5	9.719	5.70E+03	2.00E+03	7.19	3.97	(19)
^{55}Cr	0.0	6.246	6.00E+04	9.00E+03	7.67	4.23	(20)
^{56}Mn	2.5	7.271	2.70E+03	4.00E+02	7.42	4.06	(18)
^{55}Fe	0.0	9.298	2.00E+04	3.50E+03	6.50	3.41	(20)
^{57}Fe	0.0	7.646	2.50E+04	4.00E+03	7.47	4.09	(20)
^{58}Fe	0.5	10.045	5.90E+03	1.50E+03	7.55	4.20	(18)
^{59}Fe	0.0	6.581	3.50E+04	1.50E+04	8.13	4.50	(18)
^{60}Co	3.5	7.491	1.40E+03	2.00E+02	8.01	4.45	(24)
^{61}Co	5.0	9.321	3.60E+02	2.40E+01	9.34	5.57	(19)
^{59}Ni	0.0	9.000	1.37E+04	2.00E+03	7.14	3.87	(18)
^{60}Ni	1.5	11.399	1.40E+03	3.00E+02	7.47	4.16	(19)
^{61}Ni	0.0	7.820	1.60E+04	2.50E+03	7.91	4.46	(18)
^{62}Ni	1.5	10.597	1.40E+03	2.00E+02	8.05	4.58	(19)

^{201}Hg	0.0	6.230	1.30E+03	1.00E+02	16.57	8.49	(23)
^{202}Hg	1.5	7.755	1.10E+02	2.00E+01	16.75	8.85	(23)
^{203}Hg	0.0	5.933	2.50E+03	1.30E+03	16.19	8.01	(21)
^{204}Tl	0.5	6.656	3.60E+02	5.00E+01	15.15	7.51	(18)
^{206}Tl	0.5	6.503	4.00E+03	1.50E+03	12.13	4.71	(7)
^{205}Pb	0.0	6.732	2.70E+03	6.00E+02	14.46	6.69	(7)
^{207}Pb	0.0	6.738	2.40E+04	4.00E+03	11.44	3.93	(23)
^{208}Pb	0.5	7.368	1.90E+04	6.00E+03	11.04	3.47	(21)
^{209}Pb	0.0	3.937	3.50E+05	1.50E+05	12.45	3.71	(19)
^{210}Bi	4.5	4.605	4.50E+03	6.00E+02	13.15	4.88	(18)
^{227}Ra	0.0	4.561	4.88E+01	1.04E+01	30.41	19.03	(24)
^{230}Th	2.5	6.793	5.30E-01	1.50E-01	29.54	19.09	(18)
^{231}Th	0.0	5.118	9.60E+00	1.30E+00	31.42	20.21	(18)
^{233}Th	0.0	4.786	1.90E+01	6.00E+00	31.68	20.14	(19)
^{232}Pa	1.5	5.570	4.50E-01	7.00E-02	29.78	19.39	(18)
^{234}Pa	1.5	5.220	5.90E-01	9.00E-02	30.87	20.13	(18)
^{235}Pa	0.0	6.090	6.90E-01	9.00E-02	32.70	21.86	(24)
^{233}U	0.0	5.744	4.60E+00	7.00E-01	30.03	19.33	(18)
^{234}U	2.5	6.843	5.50E-01	5.00E-02	29.26	18.79	(18)
^{235}U	0.0	5.298	1.06E+01	5.00E+00	30.26	19.22	(18)
^{236}U	3.5	6.545	4.40E-01	6.00E-02	30.66	19.80	(18)
^{237}U	0.0	5.126	1.54E+01	1.00E+00	30.34	19.12	(18)
^{238}U	0.5	6.153	3.50E+00	8.00E-01	30.65	19.58	(18)
^{239}U	0.0	4.806	2.08E+01	2.00E+00	31.44	19.82	(18)
^{238}Np	2.5	5.488	5.20E-01	4.00E-02	29.14	18.63	(18)
^{239}Pu	0.0	5.647	9.00E+00	7.00E-01	28.99	18.22	(18)
^{240}Pu	0.5	6.534	2.30E+00	1.00E-01	29.79	19.00	(18)
^{241}Pu	0.0	5.242	1.36E+01	4.00E-01	30.09	18.90	(18)
^{242}Pu	2.5	6.310	9.00E-01	1.00E-01	30.75	19.65	(18)
^{243}Pu	0.0	5.034	1.75E+01	2.10E+00	30.61	19.18	(19)
^{245}Pu	0.0	4.699	2.40E+01	5.00E+00	31.69	19.84	(24)
^{242}Am	2.5	5.539	5.50E-01	1.30E-01	28.89	18.36	(18)
^{243}Am	1.0	6.364	4.00E-01	8.00E-02	30.42	19.79	(18)
^{244}Am	2.5	5.366	6.00E-01	6.00E-02	29.46	18.74	(18)
^{243}Cm	0.0	5.695	1.28E+01	2.70E+00	28.03	17.33	(20)
^{244}Cm	2.5	6.800	8.10E-01	1.00E-01	28.67	18.05	(20)
^{245}Cm	0.0	5.522	1.20E+01	1.00E+00	29.06	18.09	(18)
^{246}Cm	0.5	6.456	1.90E+00	8.00E-01	30.69	19.64	(19)
^{247}Cm	0.0	5.156	3.20E+01	5.00E+00	28.54	17.36	(20)
^{248}Cm	4.5	6.212	1.40E+00	3.00E-01	29.32	18.15	(18)
^{249}Cm	0.0	4.714	3.30E+01	5.00E+00	30.95	19.11	(18)
^{250}Bk	3.5	4.967	1.00E+00	1.00E-01	29.73	18.61	(18)
^{250}Cf	4.5	6.622	7.00E-01	1.00E-01	29.01	18.08	(18)
^{253}Cf	0.0	4.805	2.70E+01	4.00E+00	31.08	19.22	(18)

^{164}Dy	2.5	7.658	5.00E+00	8.00E-01	21.21	13.24	(18)
^{165}Dy	0.0	5.716	1.70E+02	2.50E+01	21.01	12.67	(18)
^{166}Ho	3.5	6.244	2.70E+00	5.00E-01	21.16	13.21	(24)
^{163}Er	0.0	6.902	8.00E+00	1.10E+00	23.08	15.02	(19)
^{165}Er	0.0	6.650	2.30E+01	3.00E+00	21.90	13.83	(20)
^{167}Er	0.0	6.436	4.30E+01	4.30E+00	21.43	13.27	(19)
^{168}Er	3.5	7.771	3.00E+00	5.00E-01	21.49	13.40	(5)
^{169}Er	0.0	6.003	9.40E+01	1.00E+01	21.32	12.97	(18)
^{171}Er	0.0	5.682	1.50E+02	1.50E+01	21.52	12.96	(24)
^{170}Tm	0.5	6.593	6.00E+00	1.00E+00	21.03	13.17	(22)
^{169}Yb	0.0	6.867	2.26E+01	1.30E+00	21.41	13.37	(20)
^{171}Yb	0.0	6.615	2.30E+01	3.00E+00	22.14	13.88	(19)
^{172}Yb	0.5	8.020	5.80E+00	5.00E-01	21.79	13.73	(18)
^{173}Yb	0.0	6.367	6.30E+01	3.00E+00	21.04	12.78	(19)
^{174}Yb	2.5	7.464	7.80E+00	9.00E-01	21.04	12.82	(18)
^{175}Yb	0.0	5.822	1.62E+02	1.80E+01	20.97	12.48	(18)
^{177}Yb	0.0	5.567	1.85E+02	2.00E+01	21.62	12.89	(18)
^{176}Lu	3.5	6.293	2.10E+00	2.70E-01	21.70	13.52	(19)
^{177}Lu	7.0	7.072	1.30E+00	1.80E-01	22.48	14.00	(19)
^{175}Hf	0.0	6.709	1.60E+01	3.00E+00	22.18	13.94	(19)
^{177}Hf	0.0	6.384	3.20E+01	7.00E+00	22.36	13.89	(18)
^{178}Hf	3.5	7.626	2.40E+00	3.00E-01	22.42	14.01	(18)
^{179}Hf	0.0	6.100	5.30E+01	7.40E+00	22.33	13.71	(19)
^{180}Hf	4.5	7.388	3.80E+00	3.80E-01	22.09	13.55	(18)
^{181}Hf	0.0	5.696	1.00E+02	4.00E+01	22.49	13.63	(19)
^{181}Ta	8.0	7.577	1.10E+00	1.00E-01	21.28	13.01	(18)
^{182}Ta	3.5	6.063	4.30E+00	3.00E-01	21.19	12.87	(18)
^{183}Ta	3.0	6.934	3.60E+00	7.20E-01	21.55	13.20	(19)
^{181}W	0.0	6.683	1.80E+01	4.00E+00	22.72	14.24	(19)
^{183}W	0.0	6.191	5.00E+01	1.20E+01	22.22	13.58	(5)
^{184}W	0.5	7.412	1.20E+01	1.00E+00	22.38	13.87	(18)
^{185}W	0.0	5.754	8.70E+01	8.70E+00	22.65	13.76	(19)
^{187}W	0.0	5.466	1.25E+02	9.00E+00	22.98	13.88	(24)
^{186}Re	2.5	6.178	3.30E+00	3.00E-01	21.80	13.43	(18)
^{188}Re	2.5	5.872	3.50E+00	4.20E-01	22.64	14.04	(19)
^{187}Os	0.0	6.291	3.00E+01	6.00E+00	22.95	14.22	(7)
^{188}Os	0.5	7.989	4.40E+00	2.00E-01	22.57	14.21	(18)
^{189}Os	0.0	5.922	4.00E+01	2.00E+00	23.70	14.72	(18)
^{190}Os	1.5	7.793	3.30E+00	2.00E-01	22.48	14.02	(18)
^{191}Os	0.0	5.758	7.00E+01	5.00E+00	23.18	14.16	(18)
^{193}Os	0.0	5.584	1.15E+02	1.00E+01	22.83	13.74	(18)
^{192}Ir	1.5	6.212	3.30E+00	3.00E-01	22.52	14.03	(20)
^{193}Ir	4.0	7.757	6.30E-01	1.00E-01	22.21	13.93	(20)
^{194}Ir	1.5	6.067	7.70E+00	8.00E-01	21.41	12.96	(24)
^{195}Pt	0.0	6.105	2.40E+02	7.50E+01	19.73	11.34	(18)
^{196}Pt	0.5	7.922	1.80E+01	3.00E+00	20.37	12.23	(18)
^{197}Pt	0.0	5.846	3.80E+02	1.00E+02	19.66	11.14	(20)
^{198}Au	1.5	6.512	1.62E+01	3.00E-01	19.07	11.08	(18)
^{200}Hg	0.5	8.029	8.40E+01	1.80E+01	17.63	9.75	(19)

^{133}Xe	0.0	6.447	7.50E+02	2.30E+01	15.71	9.17	(19)
^{136}Xe	1.5	7.993	5.00E+02	1.00E+02	13.27	7.05	(23)
^{134}Cs	3.5	6.892	2.00E+01	2.00E+00	15.75	9.40	(18)
^{135}Cs	4.0	8.827	1.30E+01	2.40E+00	14.66	8.59	(19)
^{137}Cs	5.0	8.272	5.80E+01	1.20E+01	13.44	7.32	(24)
^{131}Ba	0.0	7.493	6.60E+01	7.00E+00	17.31	10.82	(18)
^{133}Ba	0.0	7.190	1.35E+02	3.30E+01	16.87	10.34	(18)
^{135}Ba	0.0	6.973	3.80E+02	1.00E+02	15.74	9.25	(23)
^{136}Ba	1.5	9.107	3.50E+01	9.00E+00	15.16	8.96	(18)
^{137}Ba	0.0	6.899	9.20E+02	2.00E+02	14.58	8.16	(20)
^{138}Ba	1.5	8.611	2.00E+02	6.50E+01	13.59	7.42	(19)
^{139}Ba	0.0	4.723	1.40E+04	4.00E+03	14.94	7.75	(21)
^{139}La	5.0	8.778	2.10E+01	3.00E+00	14.10	7.95	(19)
^{140}La	3.5	5.161	2.40E+02	1.00E+01	15.53	8.63	(18)
^{137}Ce	0.0	7.482	1.00E+02	1.30E+01	16.51	10.04	(19)
^{141}Ce	0.0	5.429	3.00E+03	1.00E+03	15.92	8.83	(18)
^{142}Pr	2.5	5.843	6.50E+01	1.50E+01	16.48	9.67	(21)
^{143}Nd	0.0	6.124	6.63E+02	7.00E+01	16.86	9.85	(20)
^{144}Nd	3.5	7.817	3.65E+01	4.00E+00	16.87	9.98	(20)
^{145}Nd	0.0	5.755	5.40E+02	6.50E+01	18.23	10.84	(24)
^{146}Nd	3.5	7.565	1.70E+01	1.60E+00	18.77	11.49	(20)
^{147}Nd	0.0	5.292	3.30E+02	4.00E+01	20.68	12.74	(19)
^{148}Nd	2.5	7.333	5.00E+00	2.00E+00	22.02	14.27	(18)
^{149}Nd	0.0	5.039	1.67E+02	2.10E+01	23.10	14.68	(18)
^{151}Nd	0.0	5.335	1.74E+02	2.00E+01	22.09	13.83	(18)
^{148}Pm	3.5	5.894	5.70E+00	1.50E+00	20.34	12.85	(19)
^{148}Sm	3.5	8.141	5.70E+00	5.00E-01	19.22	12.01	(18)
^{150}Sm	3.5	7.986	2.50E+00	2.50E-01	21.07	13.53	(19)
^{151}Sm	0.0	5.597	6.80E+01	1.00E+01	23.02	14.79	(24)
^{152}Sm	3.5	8.258	1.30E+00	2.00E-01	21.47	13.92	(18)
^{153}Sm	0.0	5.868	6.00E+01	2.00E+01	22.32	14.21	(23)
^{155}Sm	0.0	5.807	1.30E+02	1.30E+01	21.00	12.96	(19)
^{152}Eu	2.5	6.305	8.50E-01	1.40E-01	22.98	15.28	(21)
^{153}Eu	3.0	8.553	2.50E-01	4.00E-02	21.54	14.27	(20)
^{154}Eu	2.5	6.442	1.30E+00	2.00E-01	21.96	14.32	(18)
^{155}Eu	3.0	8.152	9.20E-01	1.70E-01	20.27	12.98	(20)
^{156}Eu	2.5	6.336	4.80E+00	4.00E-01	20.04	12.51	(20)
^{153}Gd	0.0	6.247	1.50E+01	2.00E+00	23.06	15.14	(18)
^{155}Gd	0.0	6.435	1.55E+01	1.50E+00	23.12	15.10	(18)
^{156}Gd	1.5	8.536	1.60E+00	1.60E-01	21.37	13.85	(19)
^{157}Gd	0.0	6.360	4.40E+01	5.00E+00	21.39	13.46	(19)
^{158}Gd	1.5	7.937	4.90E+00	4.00E-01	21.02	13.32	(18)
^{159}Gd	0.0	5.943	8.60E+01	4.00E+00	21.48	13.34	(18)
^{161}Gd	0.0	5.635	2.02E+02	2.00E+01	20.86	12.61	(18)
^{160}Tb	1.5	6.260	3.50E+00	1.50E+00	21.13	13.43	(19)
^{159}Dy	0.0	6.831	3.00E+01	6.00E+00	20.81	13.05	(7)
^{161}Dy	0.0	6.453	2.73E+01	1.70E+00	22.12	14.06	(18)
^{162}Dy	2.5	8.197	2.00E+00	1.20E+00	21.34	13.58	(19)
^{163}Dy	0.0	6.271	6.46E+01	9.00E+00	21.08	13.01	(18)

Iljinov et al. Table 1

^{100}Ru	2.5	9.673	3.40E+01	7.00E+00	13.46	8.28	(7)
^{102}Ru	2.5	9.220	1.80E+01	2.00E+00	15.05	9.57	(20)
^{103}Ru	0.0	6.232	5.50E+02	1.50E+02	15.95	10.01	(19)
^{104}Ru	2.5	8.909	7.50E+00	3.80E+00	16.92	11.15	(20)
^{104}Rh	0.5	7.000	3.70E+01	4.00E+00	15.45	9.91	(19)
^{105}Pd	0.0	7.094	2.40E+02	3.00E+01	15.51	9.79	(19)
^{106}Pd	2.5	9.562	1.33E+01	1.70E+00	14.95	9.46	(5)
^{107}Pd	0.0	6.535	2.70E+02	9.00E+01	16.56	10.54	(20)
^{108}Pd	2.5	9.219	1.20E+01	2.00E+00	15.68	10.00	(19)
^{109}Pd	0.0	6.154	2.00E+02	8.00E+01	18.06	11.72	(20)
^{111}Pd	0.0	5.750	3.60E+02	4.70E+01	18.13	11.84	(19)
^{108}Ag	0.5	7.270	3.10E+01	6.00E+00	15.37	9.81	(5)
^{110}Ag	0.5	6.809	2.20E+01	4.00E+00	16.75	10.92	(5)
^{107}Cd	0.0	7.930	1.35E+02	3.50E+01	14.90	9.35	(18)
^{109}Cd	0.0	7.347	1.20E+02	3.00E+01	16.15	10.32	(18)
^{111}Cd	0.0	6.975	1.55E+02	2.00E+01	16.58	10.58	(18)
^{112}Cd	0.5	9.399	2.60E+01	4.00E+00	15.66	9.98	(19)
^{113}Cd	0.0	6.540	2.00E+02	4.00E+01	17.19	10.96	(18)
^{114}Cd	0.5	9.043	2.70E+01	3.50E+00	16.26	10.40	(19)
^{115}Cd	0.0	6.141	2.35E+02	3.50E+01	17.95	11.47	(18)
^{117}Cd	0.0	5.768	3.90E+02	9.00E+01	18.12	11.65	(18)
^{114}In	4.5	7.275	7.80E+00	1.10E+00	15.82	9.97	(19)
^{116}In	4.5	6.784	1.07E+01	6.00E -01	16.29	10.25	(18)
^{113}Sn	0.0	7.746	1.57E+02	5.20E+01	15.15	9.48	(20)
^{115}Sn	0.0	7.546	2.30E+02	8.00E+01	15.00	9.25	(19)
^{116}Sn	0.5	9.563	4.40E+01	2.20E+01	14.73	9.14	(19)
^{117}Sn	0.0	6.945	3.80E+02	1.30E+02	15.40	9.43	(19)
^{118}Sn	0.5	9,327	4.50E+01	1.00E+01	15.10	9.39	(19)
^{119}Sn	0.0	6.486	6.00E+02	1.50E+02	15.66	9.52	(19)
^{120}Sn	0.5	9.107	6.20E+01	1.20E+01	15.05	9.26	(19)
^{121}Sn	0.0	6.172	1.00E+03	3.00E+02	15.54	9.27	(21)
^{123}Sn	0.0	5.946	1.60E+03	8.00E+02	15.34	8.97	(21)
^{125}Sn	0.0	5.733	2.50E+03	1.20E+03	15.13	8.66	(7)
^{122}Sb	2.5	6.807	1.80E+01	2.00E+00	16.01	10.01	(18)
^{124}Sb	3.5	6.467	2.40E+01	2.40E+00	16.04	9.88	(19)
^{123}Te	0.0	6.934	1.40E+02	5.00E+01	17.14	10.88	(18)
^{124}Te	0.5	9.425	1.80E+01	4.00E+00	16.31	10.39	(19)
^{125}Te	0.0	6.571	2.20E+02	5.00E+01	17.23	10.82	(21)
^{126}Te	0.5	9.114	3.80E+01	3.00E+00	15.82	9.83	(18)
^{127}Te	0.0	6.291	6.00E+02	1.00E+02	16.27	9.81	(19)
^{129}Te	0.0	6.086	2.00E+03	6.00E+02	14.81	8.39	(21)
^{131}Te	0.0	5.930	5.70E+03	8.00E+02	13.53	7.14	(23)
^{128}I	2.5	6.826	1.90E+01	5.00E+00	16.06	9.91	(23)
^{130}I	3.5	6.463	2.70E+01	5.00E+00	16.03	9.72	(5)
^{125}Xe	0.0	7.603	6.30E+01	3.00E+00	17.03	10.87	(19)
^{129}Xe	0.0	6.908	2.60E+02	1.60E+01	16.33	9.98	(19)
^{130}Xe	0.5	9.255	3.20E+01	3.00E+00	15.86	9.82	(20)
^{131}Xe	0.0	6.616	1.90E+02	6.00E+01	17.55	10.96	(18)
^{132}Xe	1.5	8.936	4.00E+01	1.50E+01	15.22	9.07	(21)

^{63}Ni	0.0	6.839	1.91E+04	3.60E+03	8.71	5.03	(18)
^{65}Ni	0.0	6.098	2.85E+04	6.00E+03	9.14	5.26	(7)
^{64}Cu	1.5	7.916	6.90E+02	7.00E+01	8.73	5.13	(19)
^{66}Cu	1.5	7.066	1.00E+03	2.00E+02	9.16	5.46	(24)
^{65}Zn	0.0	7.980	3.60E+03	1.00E+03	9.51	5.72	(18)
^{67}Zn	0.0	7.052	6.50E+03	1.00E+03	9.90	6.02	(21)
^{68}Zn	2.5	10.198	2.90E+02	3.00E+01	9.88	6.07	(19)
^{69}Zn	0.0	6.482	8.60E+03	1.20E+03	10.35	6.28	(21)
^{71}Zn	0.0	5.834	6.90E+03	1.00E+03	11.73	7.29	(18)
^{70}Ga	1.5	7.654	2.30E+02	5.50E+01	10.34	6.49	(24)
^{72}Ga	1.5	6.521	3.70E+02	7.00E+01	11.13	7.04	(7)
^{71}Ge	0.0	7.416	2.00E+03	8.00E+02	11.06	6.99	(23)
^{73}Ge	0.0	6.782	2.20E+03	3.10E+02	11.89	7.61	(19)
^{74}Ge	4.5	10.200	9.30E+01	1.00E+01	11.26	7.06	(19)
^{75}Ge	0.0	6.506	3.90E+03	7.70E+02	11.61	7.12	(19)
^{77}Ge	0.0	6.072	8.00E+03	8.00E+02	11.41	6.77	(23)
^{76}As	1.5	7.327	9.50E+01	1.00E+01	11.95	7.75	(19)
^{75}Se	0.0	8.028	4.20E+02	2.40E+02	12.37	8.14	(18)
^{77}Se	0.0	7.419	7.90E+02	1.60E+02	12.46	8.08	(19)
^{78}Se	0.5	10.498	1.10E+02	2.00E+01	11.76	7.49	(19)
^{79}Se	0.0	6.962	1.75E+03	3.20E+02	12.10	7.49	(19)
^{81}Se	0.0	6.701	3.50E+03	1.50E+03	11.62	6.94	(18)
^{83}Se	0.0	5.818	6.90E+03	1.10E+03	11.97	7.07	(7)
^{80}Br	1.5	7.892	5.40E+01	5.00E+00	12.10	7.71	(19)
^{82}Br	1.5	7.593	9.40E+01	1.50E+01	11.84	7.37	(18)
^{79}Kr	0.0	8.362	2.30E+02	6.00E+01	12.80	8.45	(18)
^{81}Kr	0.0	7.876	2.80E+02	1.40E+01	13.28	8.66	(19)
^{83}Kr	0.0	7.463	3.82E+02	2.40E+02	13.56	8.78	(18)
^{86}Rb	2.5	8.650	1.00E+02	2.00E+01	10.47	6.10	(24)
^{88}Rb	1.5	6.083	1.60E+03	4.20E+02	10.42	5.78	(19)
^{85}Sr	0.0	8.531	4.00E+02	1.50E+02	12.06	7.55	(18)
^{87}Sr	0.0	8.428	1.00E+03	3.00E+02	11.13	6.59	(24)
^{88}Sr	4.5	11.113	1.21E+02	1.30E+01	10.05	5.62	(23)
^{89}Sr	0.0	6.365	1.20E+04	2.00E+03	10.67	5.86	(18)
^{90}Y	0.5	6.857	1.20E+03	2.00E+02	10.66	6.06	(24)
^{91}Zr	0.0	7.195	6.40E+03	1.10E+03	10.45	5.73	(18)
^{92}Zr	2.5	8.635	3.00E+02	8.00E+01	11.99	7.07	(21)
^{93}Zr	0.0	6.734	2.60E+03	7.00E+02	12.29	7.24	(18)
^{95}Zr	0.0	6.463	2.50E+03	4.00E+02	12.88	7.59	(5)
^{97}Zr	0.0	5.579	3.00E+03	8.00E+02	14.43	8.62	(21)
^{94}Nb	4.5	7.230	7.40E+01	1.00E+01	12.47	7.44	(19)
^{93}Mo	0.0	8.067	1.80E+03	3.00E+02	10.99	6.25	(19)
^{95}Mo	0.0	7.367	1.15E+03	3.50E+02	12.52	7.48	(20)
^{96}Mo	2.5	9.154	9.10E+01	1.10E+01	12.87	7.79	(20)
^{97}Mo	0.0	6.821	9.80E+02	1.40E+02	13.70	8.33	(19)
^{98}Mo	2.5	8.643	7.80E+01	1.00E+01	13.89	8.54	(19)
^{99}Mo	0.0	5.926	9.70E+02	2.20E+02	15.62	9.77	(18)
^{101}Mo	0.0	5.399	7.00E+02	5.00E+01	17.67	11.32	(20)
^{100}Tc	4.5	6.764	2.60E+01	5.00E+00	15.07	9.46	(23)

Iljinov et al. Table 1

TABLE II: Nuclear level density data for a larger interval of excitation energy.

Nuclide	E* [MeV]	ρ [MeV]	Δρ [MeV]	a_{exp}[MeV $^{-1}$] I	II	Ref.
^{22}Ne	7.000	7.00E+00	1.40E+00	4.53	2.88	(33)
^{22}Ne	8.000	1.20E+01	2.50E+00	4.30	2.60	(33)
^{23}Ne	4.500	5.00E+00	1.00E+00	4.22	2.52	(33)
^{23}Na	5.500	6.00E+00	1.20E+00	3.65	1.70	(33)
^{23}Na	6.500	1.30E+01	2.50E+00	3.83	1.94	(33)
^{23}Na	7.500	2.00E+01	4.00E+00	3.70	1.83	(33)
^{23}Na	10.050	3.68E+01	7.40E+00	3.21	1.37	(33)
^{23}Na	11.200	7.30E+01	1.50E+01	3.32	1.52	(33)
^{24}Na	2.000	4.00E+00	8.00E-01	4.16	2.16	(33)
^{24}Na	2.500	5.00E+00	1.00E+00	4.00	2.00	(33)
^{24}Na	3.000	7.50E+00	1.70E+00	4.09	2.11	(33)
^{24}Na	3.500	1.10E+01	2.40E+00	4.15	2.20	(33)
^{24}Na	4.550	3.15E+01	6.00E+00	4.51	2.63	(33)
^{24}Na	7.080	6.71E+01	1.70E+01	3.88	2.03	(33)
^{24}Na	9.250	8.40E+02	3.50E+02	4.86	3.09	(25)
^{24}Na	11.250	3.50E+02	1.50E+02	3.66	1.88	(25)
^{25}Na	5.000	1.00E+01	2.00E+00	4.66	2.95	(33)
^{24}Mg	7.500	5.00E+00	1.00E+00	3.62	1.53	(33)
^{24}Mg	8.000	8.00E+00	1.60E+00	3.80	1.77	(33)
^{24}Mg	11.440	2.18E+01	7.60E+00	3.13	1.15	(33)
^{24}Mg	12.650	4.88E+01	1.60E+01	3.30	1.40	(33)
^{24}Mg	19.900	3.23E+02	1.60E+02	2.84	0.93	(33)
^{24}Mg	25.000	1.84E+03	9.20E+02	2.89	1.07	(33)
^{25}Mg	5.000	7.00E+00	1.40E+00	4.21	2.13	(33)
^{25}Mg	6.000	1.35E+01	3.90E+00	4.19	2.16	(33)
^{25}Mg	7.150	2.19E+01	4.40E+00	3.97	1.97	(33)
^{25}Mg	12.800	3.80E+02	1.90E+02	3.90	2.06	(33)
^{25}Mg	15.100	1.10E+03	5.50E+02	3.92	2.12	(33)
^{25}Mg	17.400	2.40E+03	1.20E+03	3.82	2.05	(33)
^{25}Mg	18.600	5.30E+03	2.60E+03	3.97	2.22	(33)
^{26}Mg	6.500	6.00E+00	1.20E+00	4.65	2.85	(33)
^{26}Mg	7.000	1.20E+01	2.00E+00	5.06	3.29	(33)
^{26}Mg	11.450	6.23E+01	1.40E+01	3.85	2.04	(33)
^{27}Mg	5.000	9.00E+00	2.00E+00	4.53	2.48	(33)
^{27}Mg	5.500	1.30E+01	2.50E+00	4.53	2.50	(33)
^{26}Al	3.000	7.00E+00	1.40E+00	4.09	2.20	(33)
^{26}Al	4.550	1.59E+01	4.60E+00	3.92	2.05	(33)
^{26}Al	5.600	2.95E+01	7.40E+00	3.92	2.09	(33)
^{26}Al	7.110	5.18E+01	8.80E+00	3.73	1.90	(33)

^{26}Al	15.200	1.11E+03	5.50E+02	3.46	1.72	(33)
^{27}Al	5.000	9.00E+00	1.80E+00	4.53	2.59	(33)
^{27}Al	5.500	1.10E+01	2.00E+00	4.34	2.40	(33)
^{27}Al	7.000	2.00E+01	4.00E+00	3.98	2.04	(33)
^{27}Al	9.720	5.59E+01	8.40E+00	3.63	1.73	(33)
^{27}Al	10.500	9.34E+01	1.60E+01	3.72	1.85	(33)
^{27}Al	20.000	3.70E+03	1.80E+03	3.57	1.80	(33)
^{27}Al	21.000	1.33E+04	6.70E+03	3.98	2.26	(33)
^{28}Al	3.000	8.00E+00	1.60E+00	4.32	2.08	(33)
^{28}Al	4.000	1.50E+01	3.00E+00	4.26	2.08	(33)
^{28}Al	5.350	2.42E+01	4.60E+00	3.93	1.80	(33)
^{28}Al	6.500	4.00E+00	8.00E–01	4.02	1.88	(33)
^{28}Al	7.830	7.57E+01	2.20E+01	3.78	1.73	(33)
^{28}Al	13.100	1.06E+03	5.03E+02	3.90	1.98	(33)
^{28}Al	15.100	1.20E+03	6.00E+02	3.54	1.61	(33)
^{29}Al	4.500	7.00E+00	1.40E+00	4.70	2.35	(33)
^{29}Al	5.000	1.00E+01	2.00E+00	4.67	2.36	(33)
^{28}Si	7.000	5.00E+00	1.00E+00	3.89	1.76	(33)
^{28}Si	7.500	4.00E+00	8.00E–01	3.32	1.05	(33)
^{28}Si	8.000	5.00E+00	1.00E+00	3.28	1.03	(33)
^{28}Si	8.500	7.00E+00	1.40E+00	3.34	1.17	(33)
^{28}Si	9.000	1.00E+01	2.00E+00	3.42	1.30	(33)
^{28}Si	12.450	5.58E+01	9.50E+00	3.43	1.44	(33)
^{28}Si	19.600	7.81E+02	3.90E+02	3.28	1.38	(33)
^{28}Si	20.800	1.42E+03	7.10E+02	3.36	1.49	(33)
^{28}Si	24.550	2.24E+03	1.12E+03	3.02	1.08	(33)
^{28}Si	28.000	8.14E+03	4.10E+03	3.11	1.23	(33)
^{29}Si	4.500	5.00E+00	1.00E+00	4.24	2.05	(33)
^{29}Si	7.080	1.97E+01	3.90E+00	3.94	1.84	(33)
^{29}Si	9.310	7.21E+01	1.20E+01	3.98	1.97	(33)
^{29}Si	14.400	1.20E+02	6.00E+01	3.01	0.81	(33)
^{29}Si	16.300	5.00E+02	2.50E+02	3.29	1.31	(33)
^{29}Si	18.700	2.00E+03	1.00E+03	3.52	1.62	(33)
^{29}Si	20.300	4.00E+03	2.00E+03	3.57	1.69	(33)
^{29}Si	21.000	7.00E+03	3.50E+03	3.71	1.85	(33)
^{29}Si	21.400	7.30E+03	3.70E+03	3.66	1.80	(33)
^{30}Si	6.500	7.00E+00	1.40E+00	4.71	2.46	(33)
^{30}Si	7.000	1.20E+01	2.50E+00	4.91	2.71	(33)
^{30}Si	9.250	2.22E+01	6.40E+00	3.96	1.80	(33)
^{31}Si	5.000	7.00E+00	1.40E+00	4.24	1.88	(33)
^{31}Si	5.500	1.20E+01	2.50E+00	4.46	2.17	(33)
^{30}P	2.500	4.00E+00	8.00E–01	3.95	1.56	(33)
^{30}P	3.000	5.00E+00	1.00E+00	3.84	1.47	(33)
^{30}P	4.000	1.10E+01	2.00E+00	4.00	1.75	(33)
^{30}P	4.700	1.40E+01	2.80E+00	3.83	1.60	(33)
^{30}P	7.430	3.87E+01	7.70E+00	3.50	1.32	(33)

Iljinov et al. TABLE II

^{30}P	15.700	1.17E+03	5.80E+02	3.45	1.45	(33)
^{31}P	5.000	8.00E+00	1.60E+00	4.40	2.06	(33)
^{31}P	5.500	1.20E+01	2.50E+00	4.46	2.16	(33)
^{31}P	6.000	1.50E+01	3.00E+00	4.33	2.06	(33)
^{31}P	6.500	1.80E+01	3.00E+00	4.33	1.93	(33)
^{31}P	8.270	3.70E+01	7.40E+00	3.91	1.71	(33)
^{31}P	9.060	4.88E+01	9.80E+00	3.80	1.62	(33)
^{31}P	9.670	8.18E+01	1.60E+01	3.95	1.80	(33)
^{32}P	2.500	5.00E+00	1.00E+00	4.31	1.78	(33)
^{32}P	3.500	9.00E+00	1.80E+00	4.19	1.75	(33)
^{32}P	4.750	1.13E+01	2.30E+00	3.66	1.21	(33)
^{32}P	5.850	2.53E+01	6.30E+00	3.83	1.50	(33)
^{33}P	4.000	4.00E+00	8.00E–01	4.46	1.75	(33)
^{33}P	5.000	6.00E+00	1.00E+00	4.07	1.44	(33)
^{33}P	5.700	1.40E+01	2.50E+00	4.49	2.00	(33)
^{32}S	6.500	6.00E+00	1.00E+00	4.44	1.98	(33)
^{32}S	7.000	1.00E+01	2.00E+00	4.63	2.23	(33)
^{32}S	9.700	3.47E+01	6.90E+00	4.11	1.83	(33)
^{32}S	10.550	5.33E+01	1.30E+01	4.06	1.82	(33)
^{32}S	19.000	1.03E+03	5.10E+02	3.52	1.41	(33)
^{33}S	5.000	1.40E+01	3.00E+00	5.10	2.65	(33)
^{33}S	5.500	1.60E+01	3.00E+00	4.80	2.37	(33)
^{33}S	6.000	2.07E+01	4.10E+00	4.68	2.28	(33)
^{33}S	6.750	2.79E+01	7.00E+00	4.47	2.11	(33)
^{33}S	7.500	4.37E+01	8.70E+00	4.45	2.12	(33)
^{33}S	14.100	8.50E+02	4.25E+02	4.08	1.94	(33)
^{33}S	16.200	1.30E+03	6.50E+02	3.82	1.69	(33)
^{33}S	18.300	4.30E+03	2.10E+03	3.99	1.91	(33)
^{34}S	11.100	1.09E+02	2.00E+01	4.36	2.03	(33)
^{35}S	5.000	8.00E+00	1.60E+00	4.42	1.67	(33)
^{34}Cl	2.700	6.00E+00	1.00E+00	4.43	1.77	(33)
^{34}Cl	3.000	7.00E+00	1.40E+00	4.35	1.72	(33)
^{34}Cl	3.500	1.00E+01	2.00E+00	4.36	1.79	(33)
^{34}Cl	4.100	1.36E+01	3.40E+00	4.26	1.74	(33)
^{34}Cl	6.200	3.55E+01	6.70E+00	3.98	1.57	(33)
^{35}Cl	4.500	1.00E+01	2.00E+00	5.21	2.50	(33)
^{35}Cl	7.790	5.10E+01	8.70E+00	4.44	1.97	(33)
^{36}Cl	2.000	5.00E+00	1.00E+00	5.01	2.06	(33)
^{36}Cl	2.500	9.00E+00	1.80E+00	5.26	2.43	(33)
^{36}Cl	3.000	1.30E+01	2.50E+00	5.19	2.43	(33)
^{36}Cl	4.400	2.30E+01	5.50E+00	4.64	1.99	(33)
^{36}Cl	8.610	2.67E+02	1.40E+02	4.53	2.13	(33)
^{37}Cl	4.000	1.00E+01	2.00E+00	5.88	2.96	(33)
^{37}Cl	9.590	2.09E+02	4.20E+01	4.72	2.24	(33)
^{37}Cl	10.020	2.87E+02	3.40E+01	4.77	2.31	(33)
^{38}Cl	2.000	7.00E+00	1.40E+00	5.63	2.52	(33)

^{38}Cl	3.800	2.56E+01	5.10E+00	5.29	2.46	(33)
^{38}Cl	6.140	1.74E+02	8.40E+01	5.48	2.86	(33)
^{36}Ar	6.000	6.00E+00	1.00E+00	4.87	2.01	(33)
^{36}Ar	6.500	9.00E+00	1.80E+00	4.88	2.11	(33)
^{36}Ar	7.000	1.50E+01	3.00E+00	5.03	2.34	(33)
^{36}Ar	9.450	4.53E+01	9.10E+00	4.43	1.90	(33)
^{36}Ar	10.450	7.65E+01	1.40E+01	4.37	1.89	(33)
^{37}Ar	4.000	1.40E+01	3.00E+00	6.45	3.54	(33)
^{37}Ar	5.020	2.29E+01	5.70E+00	5.74	2.94	(33)
^{37}Ar	19.800	2.93E+04	1.50E+04	4.66	2.44	(33)
^{38}Ar	6.000	2.00E+01	4.00E+00	6.67	3.74	(33)
^{38}Ar	6.630	2.58E+01	9.00E+00	6.12	3.25	(33)
^{38}Ar	10.150	1.32E+02	2.60E+01	4.97	2.38	(33)
^{38}Ar	21.500	3.23E+04	1.62E+04	4.74	2.48	(33)
^{38}Ar	21.400	7.50E+04	3.70E+04	5.21	2.96	(26)
^{39}Ar	5.300	3.15E+01	8.50E+00	5.84	2.95	(33)
^{40}Ar	10.600	2.55E+02	5.10E+01	5.27	2.59	(33)
^{39}K	4.000	8.00E+00	1.60E+00	5.53	2.41	(33)
^{39}K	8.140	7.85E+01	1.20E+01	4.65	1.97	(33)
^{40}K	2.000	1.00E+01	2.00E+00	6.32	3.12	(33)
^{40}K	2.500	2.00E+01	4.00E+00	6.62	3.53	(33)
^{40}K	3.000	2.60E+01	5.00E+00	6.27	3.25	(33)
^{40}K	3.800	3.02E+01	6.60E+00	5.54	2.61	(33)
^{40}K	4.800	4.78E+01	1.00E+01	5.20	2.37	(33)
^{40}K	7.860	3.56E+02	7.50E+01	5.16	2.54	(33)
^{40}Ca	6.000	6.00E+00	1.00E+00	4.78	1.51	(33)
^{40}Ca	6.500	1.00E+01	2.00E+00	4.94	1.82	(33)
^{40}Ca	10.950	1.85E+02	4.40E+01	4.82	2.15	(33)
^{41}Ca	4.500	2.00E+01	6.00E+00	6.22	3.06	(8)
^{41}Ca	5.200	3.30E+01	9.00E+00	6.02	2.97	(7)
^{41}Ca	5.700	4.30E+01	1.20E+01	5.81	2.83	(7)
^{41}Ca	8.500	4.50E+02	1.30E+02	6.01	3.27	(7)
^{41}Ca	10.750	3.50E+03	1.50E+03	6.44	3.81	(25)
^{41}Ca	12.750	3.20E+03	1.30E+03	5.42	2.87	(25)
^{41}Ca	14.750	1.40E+04	6.00E+03	5.67	3.18	(25)
^{41}Ca	16.750	1.90E+04	7.00E+03	5.21	2.77	(25)
^{41}Ca	18.750	9.20E+04	3.80E+04	5.56	3.17	(25)
^{41}Ca	20.750	1.30E+05	5.00E+04	5.24	2.88	(25)
^{55}Mn	3.500	4.00E+01	1.20E+01	9.54	4.93	(7)
^{55}Mn	10.000	3.00E+03	8.00E+02	6.83	3.47	(7)
^{55}Mn	15.100	1.10E+05	3.00E+04	7.02	3.93	(27)
^{55}Mn	18.000	4.90E+05	1.50E+05	6.89	3.90	(27)
^{55}Mn	23.100	7.30E+06	2.00E+06	6.91	4.03	(27)
^{56}Fe	5.000	2.40E+01	7.00E+00	8.38	3.80	(28)
^{56}Fe	5.500	3.20E+01	9.00E+00	7.78	3.42	(28)
^{56}Fe	6.000	4.10E+01	1.20E+01	7.28	3.10	(28)

^{56}Fe	17.000	1.30E+05	3.00E+04	6.96	3.86	(28)
^{56}Fe	18.000	1.60E+05	5.00E+04	6.71	3.64	(28)
^{56}Fe	19.000	2.60E+05	7.00E+04	6.66	3.63	(28)
^{56}Fe	20.000	4.00E+05	1.20E+05	6.59	3.59	(28)
^{56}Fe	21.000	6.00E+05	2.20E+05	6.51	3.54	(28)
^{56}Fe	22.000	8.00E+05	3.00E+05	6.38	3.43	(28)
^{56}Fe	23.000	1.20E+06	4.00E+05	6.33	3.40	(28)
^{55}Co	3.550	1.09E+01	4.70E+00	6.82	2.36	(32)
^{56}Co	2.110	1.27E+01	8.10E+00	7.04	2.51	(32)
^{57}Co	3.560	3.09E+01	6.40E+00	8.81	4.18	(32)
^{58}Co	2.130	3.09E+01	1.07E+01	8.77	4.06	(32)
^{59}Co	9.600	1.70E+03	4.00E+02	6.60	3.06	(28)
^{59}Co	10.000	3.00E+03	9.00E+02	6.85	3.34	(28)
^{60}Co	2.140	3.92E+01	2.10E+01	9.28	4.41	(32)
^{60}Co	8.000	5.00E+03	1.50E+03	7.74	4.12	(7)
^{60}Co	9.500	2.90E+04	1.20E+04	8.30	4.76	(25)
^{60}Co	11.500	1.00E+05	4.00E+04	8.08	4.68	(25)
^{60}Co	13.500	2.40E+05	1.10E+05	7.70	4.41	(25)
^{61}Co	3.580	5.51E+01	1.27E+01	9.94	4.99	(32)
^{60}Ni	4.500	2.70E+01	5.40E+00	10.03	4.93	(28)
^{60}Ni	5.000	3.20E+01	6.40E+00	8.81	4.04	(28)
^{60}Ni	15.500	1.20E+05	3.60E+04	7.59	4.29	(28)
^{60}Ni	16.500	1.90E+05	5.70E+04	7.45	4.20	(28)
^{60}Ni	17.500	3.10E+05	9.00E+04	7.36	4.15	(28)
^{60}Ni	18.500	5.00E+05	2.00E+05	7.28	4.10	(28)
^{60}Ni	19.500	7.50E+05	2.20E+05	7.17	4.03	(28)
^{60}Ni	20.500	1.10E+06	3.30E+05	7.06	3.94	(28)
^{60}Ni	21.500	1.80E+06	5.40E+05	7.02	3.94	(28)
^{60}Ni	22.500	2.50E+06	7.00E+05	6.91	3.85	(28)
^{62}Ni	5.000	3.40E+01	1.00E+01	8.87	3.98	(28)
^{63}Cu	3.500	4.00E+01	7.00E+00	9.49	4.41	(28)
^{63}Cu	4.000	5.00E+01	8.00E+00	8.63	3.83	(28)
^{63}Cu	8.600	2.10E+03	6.00E+02	7.55	3.74	(28)
^{63}Cu	9.000	4.10E+03	1.20E+03	7.90	4.12	(28)
^{65}Cu	3.500	4.50E+01	9.00E+00	9.73	4.55	(28)
^{65}Cu	4.000	5.60E+01	1.60E+01	8.84	3.94	(28)
^{114}Cd	9.000	2.20E+06	6.00E+05	17.67	11.39	(29)
^{166}Ho	6.250	3.20E+06	9.00E+05	20.58	12.37	(29)
^{184}Re	9.850	7.00E+08	2.10E+08	21.11	13.46	(31)
^{197}Hg	9.200	1.23E+08	3.00E+07	21.52	13.45	(31)
^{200}Tl	10.240	6.67E+07	2.00E+07	17.29	9.84	(31)
^{209}Po	7.550	3.20E+05	1.00E+05	15.77	7.52	(31)
^{209}Po	8.800	1.92E+06	6.00E+05	16.08	8.14	(31)
^{209}Po	9.500	6.40E+06	2.00E+06	16.57	8.75	(31)
^{209}Po	11.860	1.60E+08	4.50E+07	17.22	9.77	(31)
^{230}Th	3.240	1.00E+04	2.00E+03	32.74	17.24	(30)

^{230}Th	4.670	2.00E+05	4.00E+04	28.58	16.12	(30)
^{230}Th	5.060	4.60E+05	1.60E+05	28.23	16.22	(30)
^{230}Th	5.500	1.30E+06	4.00E+05	28.28	16.65	(30)
^{230}Th	6.000	4.00E+06	1.20E+06	28.32	17.07	(30)
^{230}Th	6.820	2.00E+07	6.00E+06	28.08	17.38	(30)

Iljinov et al. TABLE II

TABLE III - Results of level density analysis for different variants of the phenomenological systematics.

α	β	γ	*f*–factor	shell corrections
Without collective effects (K_{rot}=1, K_{vib}=1)				
0.114	0.098	0.051	1.68	Myers, Swiatecki
0.111	0.107	$\tilde{a}$ /0.46$A^{4/3}$(*)	1.71	
0.072	0.257	0.059	2.31	Cameron
0.077	0.229	$\tilde{a}$ /0.037$A^{4/3}$(*)	2.48	
With collective effects ($K_{rot}\neq$1, $K_{vib}\neq$1)				
0.090	–0.040	0.070	1.63	Myers, Swiatecki
0.034	0.312	0.011	5.00(**)	
0.052	0.113	0.086	2.20	Cameron
0.029	0.332	0.012	5.47(**)	

(*) The value given is relative to the ε parameter (remember that $\gamma = \tilde{a}/\varepsilon A^{4/3}$).

(**) Nuclides with deformation $\beta < 0.2$ were assumed to be spherical (K_{rot}=1).

TABLE IV - Results of analysis of the ratio Γ_f/Γ_n for different variants of the phenomenological level density systematics.

	I VARIANT			II VARIANT			III VARIANT			IV VARIANT		
COMPOUND NUCLEUS	B_f [MeV]	a_f/a_n	δW_{sp} [MeV]	B_f [MeV]	a_f/a_n	δW_{sp} [MeV]	B_f [MeV]	a_f/a_n	δW_{sp} [MeV]	B_f [MeV]	$\tilde{a}_f/\tilde{a}_n$	δW_{sp} [MeV]
$^{173}_{71}Lu$	27.0	1.140	0	29.5	1.08	0	30.0	1.15	0	30.0	1.00	- 5.0
$^{179}_{73}Ta$	25.0	1.120	0	28.0	1.10	0	28.0	1.16	0	29.0	1.00	- 4.0
$^{188}_{76}Os$	21.5	1.09	0	24.0	1.08	0	24.0	1.13	0	25.0	1.00	- 4.5
$^{189}_{77}Ir$	20.0	1.12	0	21.5	1.07	0	21.5	1.10	0	22.5	1.00	- 4.5
$^{198}_{80}Hg$	19.5	1.08	0	21.5	1.07	0	21.0	1.10	0	23.0	1.00	- 4.0
$^{201}_{81}Tl$	20.5	1.09	0	22.5	1.08	0	22.5	1.14	0	23.0	1.00	- 5.0
$^{206}_{82}Pb$	22.0	1.05	0	24.5	1.06	-1.0	24.0	1.08	0	25.0	1.00	- 6.0
$^{209}_{83}Bi$	21.0	1.03	0	23.5	1.04	-1.0	23.0	1.05	0	23.5	1.00	- 7.0
$^{212}_{84}Po$	17.0	1.07	0	18.0	1.09	-2.0	18.5	1.09	0	17.0	1.00	-7.0
$^{213}_{85}At$	15.5	1.09	0	16.5	1.10	-1.0	17.0	1.13	0	18.0	1.00	- 4.0

TABLE V - Empirical values of the saddle point shell corrections δW^{A}_{sp} and δW^{B}_{sp} for actinides.

Z	δW MeV	δW^{B}_{sp} MeV
90	2.80	- 0.50
92	2.20	- 0.50
94	2.00	0.00
96	2.80	0.50

Z	δW^{A}_{sp} MeV	δW^{B}_{sp} MeV
91	2.80	- 0.50
93	2.20	- 0.20
95	2.50	0.50
97	2.80	0.50